Global Journal of Structural Design and Construction

Volume No. 12

Issue No. 1

January - April 2024

ENRICHED PUBLICATIONS

ENRICHED PUBLICATIONS PVT. LTD

S-9, IInd FLOOR, MLU POCKET,
MANISH ABHINAV PLAZA-II, ABOVE FEDERAL BANK,
PLOT NO-5, SECTOR-5, DWARKA, NEW DELHI, INDIA-110075,
PHONE: - + (91)-(11)-47026006

Global Journal of Structural Design and Construction

Aims and Scope

Global Journal of Structural Design and Construction is a peer reviewed journal published by Original Papers. It is one of the pioneering starts up journal in Civil and Structural engineering which receives high quality research works from researchers across the globe. The journal publishes original research and review papers falling within the broad field of Civil Engineering.

Global Journal of Structural Design and Construction

Global Journal of Structural Design and Construction

(Volume No. 12, Issue No. 1, January - April 2024)

Contents

New Designs Of Stilling Basins For Square Pipe Outlets

[1]**Arun Goel**

[1]Professor, Civil Engineering Department,N. I. T. Kurukshetra.136119.India.

E mail: drarun_goel @yahoo.co.in.

Mobile no. :+91 9416393419

ABSTRACT

This paper proposes efficient designs of stilling basins by means of laboratory experimentation as compared to USBR type VI stilling basin models. These models are tested for a 4cm x 4cm square pipe opening having inflow Froude number Fr = 6.43. Different shapes and sizes of appurtenances such as impact wall, wirenets, baffle blocks, intermediate sill, end sills and their combination are tested in the laboratory for evolving new models as compared to USBR types VI stilling basin models used for pipe outlets. The performance of each model has been compared by measuring magnitude and location of maximum depth of scour after end of stilling basin and converting it into non-dimensional number called performance number. The results indicate that there is a great improvement in the performance of the models if a wire mesh (small or large openings) is used at any location inside the basin. The results indicated that provision of intermediate sill of any shape and sloping end sill improvs the working of the stilling basin model. Introduction of a row of baffle blocks etc. play an important role in dissipating the energy of flow by creating more drag inside the basin. Finally few designs using different types of appurtenances are suggested in this paper as the outcome.

Keywords—Pipe outlets, Stilling basin, Performance, Wedge shaped blocks, USBR type VI basin.

1. INTRODUCTION

Stilling basins are frequently used to reduce the kinetic energy of flow for achieving safe flow conditions in the downstream of spillways, dams, barrages, pipe outlets etc. A number of stilling basin models for the pipe outlets have been recommended like USBR impact type VI stilling basin (Bradely & Peterka 1957), Manifold type (Fiala & Albertson 1961), New designs by Goel & Verma (1999;2006), Verma & Goel (2000;2001;2003), Goel (2008), Tiwari et al. (2011), Tiwari (2012) etc. The literature review revealed that there is no direct design of stilling basin for the pipe outlet of the square shape. The present study is aimed at suggesting new designs of basins for square shaped pipe outlets having shorter length and having higher efficiency as compared to the equivalent USBR impact type VI stilling basin for Fr = 6.43.

1.1 Design Calculations of Model

The dimensions of USBR impact type VI stilling basin model (Lancastre 1987) for a square shaped outlet of 4cm size were calculated for Fr = 6.43. If the shape of the outlet opening is other than circular, than the area of opening is converted into equivalent diameter as mentioned by Lancastre (1987) and Froude number is calculated on the basis of equivalent diameter de in place of diameter d as below:

Area of square opening (d x d) = area of equivalent circular opening $\frac{\pi}{4} d_e^{\,2}$. Substituting d = 4cm in above relation, we get equivalent diameter d_e= 4.51cm. The width of stilling basin model W is expressed as:

$$W / d_e = 3\,Fr^{0.55} \tag{1}$$

For the given values of Fr = 6.43, d_e = 4.51cm. By using above relation, basic parameters for the stilling basin for square shape pipe outlet are calculated below.

(i) Stilling basin models tested for pipe of size d = 4cm, (ii) Width of basin = 9.4d, (iii) USBR type impact wall (hood = 1.66d, height = 3.61d), (iv) gap at bottom = 1.66d (v) end sill of height = 1.66d and slope 1:1 (vi) length of basin = 10.9d, (vii) impact wall location = 4.87d, (viii) Tail water depth = 3.38d.

1.1 Wedge Shaped Baffle Blocks

The rectangular baffle blocks are provided inside the stilling basins because the rectangular shape offers maximum drag. The problem of reattachment of flow on the sides of rectangular block reduces the wake area and thereby, the drag. On the basis of experimental studies (Pillai & Unny 1964) had shown that the wedge shaped baffle block of vertex angle 120o cut back at 90o on the downstream side offers more drag due to increase in the wake area (Pillai & Jayaraman 1967; Pillai et al. 1989). A strong circulatory movement of water with vertical axis was formed on either side of the block in the cutback portion resulting in the increased wake area as shown in Figure 1. The wedge shaped baffle blocks of vertex angle 150o and cut back on sides at 90o were adopted for the development of the stilling basin.

2. EXPERIMENT FACILITY & PROCEDURE

The experiments were conducted in the Fluid Mechanics Laboratory of the N I T Kurukshetra. A 12m long, 0.60m wide and 0.90m deep flume was used to conduct the experiments. One 15 H.P. centrifugal pump was installed in the supply pipe for recirculation of flow. An erodible bed consisting of sand material passing through 2.36 mm size Indian Standard sieve and retained on 1.18mm size Indian Standard sieve was filled on the downstream of the stilling basin. The run time for each model was kept as one hour and depth of flow equal to 3.38d as recommended. The model of the required geometry of stilling basin was fabricated in the flume. The granular material for the erodible bed was filled and leveled up to the top of the end sill. The pump was switched on and flow to the flume was gradually raised according to the desired outlet Froude number. At the end of the experiment, the pump was stopped and the tailgate was closed and the water inside the flume was drained out slowly without causing any disturbance to the developed scour pattern on erodible bed. The scour parameters such as magnitude of maximum depth of scour (d_m) and its distance from the end sill (d_s) were measured by using a pointer gauge and a scale (Figure 2).

2.1 Performance Criteria

The performance of a stilling basin is a function of outlet inflow Froude number (Fr), size of square pipe outlet (d), normal tail water depth of flow (h), maximum depth of scour (d_m) and its location after the end sill (d_s). A stilling basin model resulting into smaller depth of scour at larger distance is considered to have better performance as compared to another stilling basin which results into larger depth of scour at smaller distance, when tested under similar conditions. The scour Froude number F_{dm} based on mean velocity of flow in the channel V_c and depth of maximum scour d_m can be expressed as

$$\text{Fdm} = \frac{V_c}{\sqrt{g d_m}} \qquad (2)$$

If the scour pattern is assumed to be parabolic, the value of tan is the slope of the tangent drawn to the base parabola of the depth of maximum scour downstream of the end sill as shown in Figure 2.

$$\tan\alpha = \frac{2d_m}{d_s} \qquad (3)$$

These two parameters are combined into one non-dimensional number Performance number (P N).

$$\text{P N} = \frac{F_{dm}}{\tan\alpha} = \frac{F_{dm} \times d_s}{2d_m} \qquad (4)$$

Substituting value of Fdm in the equation (3),

$$\text{Performance number P N} = 0.025 d_s \left(\frac{d}{d_m}\right)^{\frac{3}{2}} \qquad (5)$$

A higher value of performance number indicates a better performance of a stilling basin model.

3. EXPERIMENTAL SCHEME

A stilling basin model was designed and fabricated in still bed flume Froude No. Fr = 6.43. An outlet of square shape of size 4cm × 4cm was used for experimentation. The appurtenances of desired proportion were fixed on the wooden floor of the flume. The various appurtenances like a net, baffle blocks, intermediate sill and end sill have been used. Nineteen number of models were tested on 10.9d length of basin and a Froude No. Fr = 6.43 by changing the configuration of the stilling basin. The performance of basin was judged on the basis of their maximum scour depth and its distance from the end sill. The main objective of the experiment was to study the performance of the stilling basin and to see the possibility of any improvement in working of stilling basin in the length of apron equal to 10.9d. The detail of models (Table 1) is given below.

The equivalent stilling basin model of USBR impact type VI namely model no. 1 (Figure 3) with an impact wall without notch and a sloping end sill (1V: 1H) of height 1.66d was designed. Keeping in view performance of USBR model no 1, new models namely models no.2 to models no 19 were prepared and tested in the length of basin to 10.9d (Table 1). The stilling basin model no. 1 consists of an USBR type impact wall without notch and triangular end sill. The stilling basin model no. 2 consists of USBR type impact wall without notch and a rectangular end sill. The stilling basin model no. 3 consists of USBR type impact wall without notch, wedge shape blocks (four in number) and triangular end sill. The stilling basin model no. 4 consists of USBR type impact wall without notch, Trapezoidal shaped blocks (four in number) and triangular end sill. The stilling basin model no. 5 consists of USBR type impact wall without notch, wedge shape blocks (four in number) and triangular end sill. The stilling basin model no. 6 consist of USBR type impact wall without notch, rectangular blocks (four in number) and a triangular end sill. The stilling basin model no. 7 consists of USBR type impact wall without notch, rectangular blocks (four in number) and triangular end sill. The stilling basin model no. 8 consist of small size net (near the outlet), USBR type impact wall without notch and triangular end sill. The stilling basin model no. 9 consist of small size net (on hood of the impact wall), USBR type impact wall without notch and triangular end sill. The stilling basin model no. 10 consist of small size net (between the impact wall and outlet), rectangular type blocks USBR type impact wall without notch and triangular end sill. The stilling basin model no. 11 consists of USBR type impact wall without notch, small size net (between the impact wall and end sill) and triangular end sill. The stilling basin model no. 12 consists of USBR type impact wall without notch, square shaped intermediate sill and triangular end sill. The stilling basin model no. 13 consist of large size net (between the impact wall and outlet), USBR type impact wall without notch and triangular end sill. The stilling basin model no. 14 consist of large size net (on hood of the impact wall), USBR type impact wall without notch and triangular end sill. The stilling basin model no. 15 consists of USBR type impact wall without notch, large size net (between the impact wall and end sill) and triangular end sill. The stilling basin model no. 16 consists of USBR type impact wall without notch, intermediate square sill, intermediate triangular sill and triangular end sill. The stilling basin model no. 17 consists of USBR type impact wall without notch, intermediate square sill and triangular end sill. The stilling basin model no. 18 consists of USBR type impact wall without notch, intermediate square sill, intermediate triangular sill and triangular end sill. The stilling basin model no. 19 consists of USBR type impact wall without notch, intermediate square sill, intermediate triangular sill and triangular end sill.

4. ANALYSIS OF RESULTS

The values of performances are calculated for each model and are given below in Table 1. Higher value of performance number (PN) indicates a better performance of the stilling basin model. The models no. 1 to 19 were tested by using impact wall, intermediate sill, baffle block and end sill of different shapes, size and location. These are discussed below in the following paragraphs.

4.1 Use of Different End Sills

Two end sills say sloping (1V: 1H) and rectangular of same heights were used in model no. 1 and 2. The scour index values obtained are 0.307 and 0.071 respectively. The higher value (0.307) in triangular end sill represents a better end sill and the same has been in subsequent design of stilling basin models.

4.2 Use of Baffle Blocks

In models no. 3, 4, 5, 6, 7 baffle block of different shapes like wedge shape (model no. 3, 5), trapezoidal shape (model no. 4) and rectangular (model no.6, 7) were used along with a triangular end sill. The values of performance number obtained are 1.088, 1.93, 1.02, 0.247, 1.84 in models no. 3, 4, 5, 6, 7 respectively. The higher values of Performance number indicates that the performance of models has improved by provision of baffle blocks except in model no. 6 which may be wrong placement of the baffle blocks with respect to flow direction. In this series of arrangement, the model no. 4 having baffle locks of trapezoidal shape is the best performing model.

4.3 Use of Wire-Mesh Net

In models no 8, 9, 10, 11, 13, 14, 15 two types of wire mesh net were employed and tested in model no 8, 9, 10, 11 (smaller wire nets) and in models no 13, 14, 15 (larger size mesh) were tested with a sloping end sill. The calculated values of performance number are 0.0(zero scour), 0.0(zero scour), 0.70, 0.71, 0.037 and 0.89 respectively in the models 8, 9, 10, 11, 13, 14, 15. It indicates that there is a great improvement in the performance of the models if a wire mesh (small openings) as shown in models no. 8 and 9 as nearly zero scour was observed in these two cases. The small size wire mesh in models 10, 11 and large size wire mesh in model no. 15 improved the performance. But the model no. 13 and 14 with large size opening are showing poor performance which may be inappropriate placement of the mesh. The provision of very small size wire mesh created a lot of diffusion and turbulence in the flow which produce more energy dissipation. When wire mesh is placed close to the exit of outlet, the almost no scour as observed meaning thereby showing the best performance of the stilling basin models 8 and 9. The perusal of this study shows that net size and location both are quite important for dissipation of kinetic energy of flow.

4.4 Use of Intermediate Sill

An intermediate sill of different shapes like square, triangular (different slopes) were used in the models named as no. 12, 16, 17, 18 and 19. In model no. 12 only one intermediate sill is used while in models 16, 17, 18 and 19 two intermediate sills (one below the impact wall and other beyond the impact wall) were placed. The values of performance number obtained are 0.76, 0.129, 0.081, 0.201 and 0.27 in the models no. 12, 16, 17, 18 and 19 respectively. The performance number of models having two intermediate sills (model no 16, 17, 18, 19) is lower than that of one intermediate sill of square shape (model no. 12). It indicates that provision of two intermediate sills is of no use and one intermediate sill is better than two intermediate sills.

5. DISCUSSION OF RESULTS

The present experimental study on development of new designs of stilling basin models indicate that the appurtenances like impact wall, intermediate sill, a row of baffle blocks, end sills and the wire mesh net play an important role in dissipating the kinetic energy of flow. The net of small size with out gap generates very small layers inside the flow which create a lot of diffusion in the basin and resulted into loss of kinetic energy of flow. But there is fear of logging of these opening by means of sediment laden or floating debris. In that case, a wire mesh net of bigger size can be used and has been tested in the present study. The impact wall helps in spreading the jet uniformly into full width of the basin. The stronger vortices are produced in the vertical plane when the expanding jet of water strikes the impact wall. The gap below it allows a portion to move out in the forward direction. The intermediate sill creates more shear layer and friction in the flow. The introduction of baffle blocks produced more drag and turbulence in the flow of stilling basin. The end sill helps in creating the reverse roller at the end of the basin and deposits the eroded material behind it. It also assists in carrying away the high velocity filament from the erodible bed. Ultimately all these appurtenances lead to more & more dissipation of kinetic energy of the flow and helps in making the downstream bed and banks safer from failure.

6. CONCLUSIONS

A stilling basin model can be developed by using appurtenances like a wire mesh net, an impact wall, a row of baffle blocks, intermediate sill and end sill. The performance of various stilling basin models has been compared by noting the maximum scour depth and its location after the end sill in terms of a non-dimensional number called as Performance number. The working of sloping end sill is better than rectangular end sill under same flow conditions. The provision of a wire mesh net of smaller size as compared to large sixe net in front of the impact wall improves the functioning of the stilling basin. The performance of the basin improves, when a row of baffle blocks of any shape is inside the stilling basin. However, more testing of stilling basin models is required using other appurtenances within a range of Froude numbers.

Table 1 Stilling basin models tested for square pipe of size d = 4cm, Fr = 6.83, width of basin = 9.4d, USBR type impact wall (hood = 1.66d, height = 3.61d) gap at bottom 1.66d and end sill (height =1.66d, slope 1:1)

Model no.	**Baffle blocks (4 no.s)**				**Intermediate sill**			**Wire mesh net**		**P N**
	Location from exit	Shape	width	height	Location	Shape	height	Location	Size	
1	-	-	-	-	-	-	-	-	-	0.307
2	-	-	-	-	-	-	-	-	-	0.071
3	6.6d	Wedge	0.7d	0.75d	-	-	-	-		1.088
4	6.3d	Trapezoidal	0.7d	0.9d	-	-	-	-		1.93
5	6.6d	Wedge	0.84d	1.1d	-	-	-	-		1.023
6	6.7d	Rectangular	1.5d	1.5d	-	-	-	-		0.247
7	6.1d	rectangular	0.6d	1.5d	-	-	-	-		1.84
8	-	-	-	-	-	-	-	0.3d	Small	0
9	-	-	-	-	-	-	-	3d	Small	0
10	-	Rectangular	1.5d	1.5d	-	-	-	1.3d	Small	0.7

11	-	-	-	-	-	-	-	7.13d	Small	0.707
12	-	-	-	-	6.2d	square	1.55d	-	-	0.76
13	-	-	-	-	-	-	-	0.3d	Large	0.026
14	-	-	-	-	-	-	-	2.7d	Large	0.037
15	-	-	-	-	-	-	-	7.7d	large	0.888
16	-	-	-	-	5.4d, 7.8d	Square, triangular	0.6d, 0.4d	-	-	0.129
17	-	-	-	-	5.4d	square	0.6d	-	-	0.081
18	-	-	-	-	5.4d, 7.95d	Square, triangular	0.6d, 0.5d	-	-	0.201
19	-	-	-	-	5.4d, 8.43d	Square, triangular	0.6d, 0.5d	-	-	0.27

REFERENCES

Bradely, J.N., and Peterka. A.J. (1957). Hydraulic design of stilling basins(1-6 papers). Journal of Hydraulic Division, ASCE,1401-1406.

Fiala, J.R., and Albertson M. L. (1961). Manifold stilling basin. Journal of Hydraulic Div, ASCE: 87, 55-81.

Garde, R. J., Saraf, P. D., and Dahigaonkar, D. J. (1986). Evolution of design of energy dissipator for pipe outlets. J. of Irrigation and Power, Vol. 42, No. 3, 145-154.

Goel Arun and Verma, D.V.S. (1999). Improved design of energy dissipators for pipe outlets. J. of Irrigation and Drainage Systems, Kluwer Academic Pub., The Netherlands, Vol.13, No.4,313-320,

Goel Arun and Verma, D.V.S. (2006). Alternate design of energy dissipators for pipe outlets. J. of Irrigation and Drainage Systems, The Netherlands, Vol.13, No.4, 313-320,

Goel, A. (2007). Experimental study on stilling basins for square outlets. Proceeding 3rd International Conference on Applied and Theoretical Mechanics, Spain, 14-16.

Goel, A. (2008). Design of stilling basin for circular pipe outlet. Canadian Journal of Civil Engineering, Vol. 35, No. 12, 1365-1374.

Lancastre Armando (1987). Hand Book of Hydraulics Engg, Eills Horwod Ltd, Halsted Press, 208-209.

Pillai, N. N., and Unny T. E. (1964). Shapes of appurtenances in stilling basins. Journal of Hydraulic Engg. Division, ASCE: 90:1-21.

Pillai, N. N., and Jayaraman, V. V.(1967). Cavitation on baffle piers in stilling basins. Symposium on High Velocity Flow. Indian Institute of Science. Banglore.

Pillai, N. N., and Goel, Arun (1989). Hydraulic jump type stilling basins for low inflow Froude numbers. Journal of Hydraulic Division, ASCE: 115, 989-994.

Tiwari, H. L., Goel, A., and Gahlot, V. K. (2011). Evolution of stilling basin. Proc. 38th National conference on Fluid Mechanics and Fluid power, Bhopal, India. 1-8.

Tiwari, H. L. (2012). Experimental investigations of hydraulic energy dissipators for rectangular pipe outlets, PhD Thesis, MANIT Bhopal.

Verma, D.V.S., and Goel, Arun. (2000). Stilling basins for pipe outlets using wedge-shaped splitter block. Journal of Irrigation and Drainage Division, ASCE, Vol. 126, No.3, 179-184.
Verma, D.V.S., and Goel Arun (2001). Model studies on stilling basins for pipe outlets. J. of Irrigation and Drainage Systems, Kluwer Academic Publisher, The Netherlands. Vol.15, No.1, 81-91,
Verma D.V.S., & Goel, Arun. (2003). Development of efficient stilling basins for pipe outlets. Journal of Irrigation and Drainage Division, ASCE, Vol.115, No.7,194-200.
Vollmer, E. and Khader, M. H. A. (1971). "Counter current energy dissipator for conduit outlets." International J. of Water Power, Vol. 13, No. 7, 260-267.

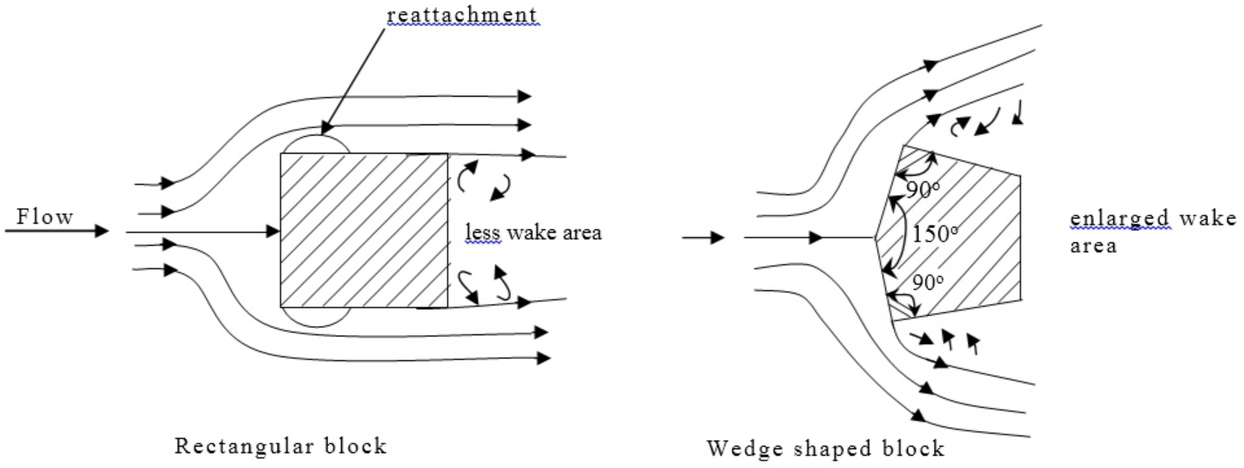

Figure 1 Comparison of wake areas

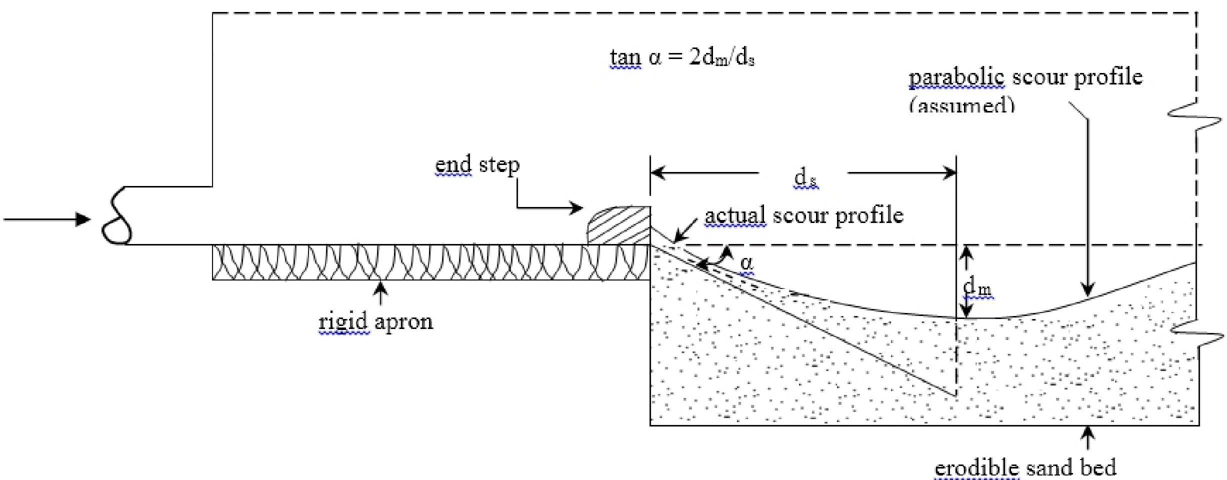

Figure 2 Scour profile

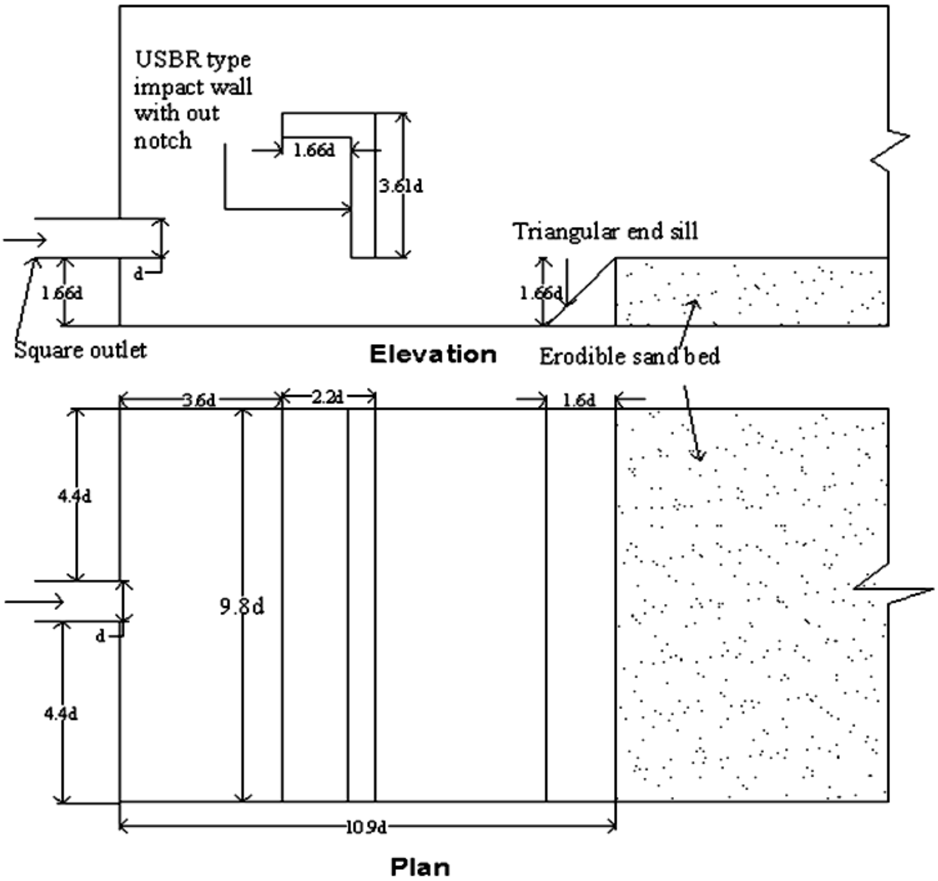

Figure 3 Stilling Basin Model No.1

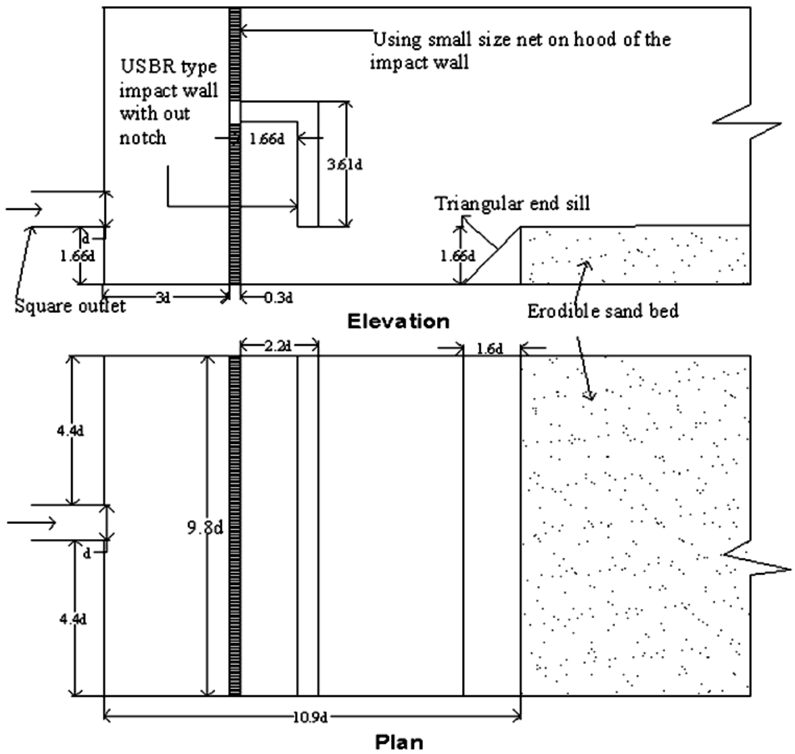

Figure 4 Stilling Basin Model No.9

Estimation Of Design Wave And Water Level Conditions For The Development Of A Port – A Case Study

Pardeshi G. R.[1] , Jagtap S. P. [2] , Dorle P. K. [3] , M. D. Kudale [4]

[1]1Research Assistant., Central Water and Power Research Station, Khadakwasala, Pune-41 024, India

[2]Assistant Research officer, Central Water and Power Research Station, Khadakwasala, Pune-41 024, India

[3] Scientist 'B', Central Water and Power Research Station, Khadakwasala, Pune-41 024, India

[4] Scientist 'E', Central Water and Power Research Station, Khadakwasala, Pune-41 024, India

Email: pardeshi .gokul@gmail.com

A B S T R A C T

The extreme wave and water level conditions are the most important parameters in the design of coastal projects like ports, nuclear power plants etc. The determination of design wave height is based on statistical analysis of extreme wave height measurements. Since the long term measured data at the site are seldom available, the extreme value analysis is usually considered using hindcast storm wave data and storm surge data. The extreme value analysis of hindcast data provides the storm surge levels and wave heights of various return periods required for the design of coastal structures. In the extreme value analysis, the wave heights for various return periods are predicted by fitting the data set to distribution functions like Gumbel, Weibull and Log- Normal distribution. The paper presents a case study for hindcasting analysis at the Nandgaon coastal region where a major port has been proposed by the Govt. of Maharashtra. Nandgaon is located at Latitude 18º 22' 33" N & Longitude 72º 55' 25" E on the northern periphery of Thane district (Fig 1). The proposed port located 7 km south of the Tarapore Point, would serve the needs of the JSW steel and power plants in the immediate hinterland, besides serving the ever increasing need of the industries located inside and beyond the MIDC area at Tarapore.

The purpose of study was to determine the extreme wave condition and storm surge for the design of breakwater for the development of port facilities. The hindcast storm wave data were obtained by considering the storms in the vicinity of the Nandgaon area between the years 1981 and 2010 (30 years). These data were analysed to find storms, which passed by the area of interest and are significant to the proposed project site. The Hydrographic Charts were use to find out length of the continental shelf and depth contours required in the analysis of storm surge. The wave conditions obtained by the studies are at the water depth of about 40 m. The storm surge and wave heights were evaluated for return periods 100– year, 50 – year and 25 – year. The analysis indicated storm surge of 3.0 m, 2.7 m and 2.3 m and significant wave height of 6.5 m, 5.8 m and 5.1 m for these return period respectively.

Keywords—Significant wave height, Storm surge, Return period.

1. INTRODUCTION

The design wave and water level condition for maritime structure is the extreme wave height that a structure should withstand without significant damages. These conditions are generally derived through hindcasting analysis of the past storms. All the storms generating wave height above a certain level, during the period of 20 to 30 years or longer are selected for the analysis. The storm wave data is then fitted to the selected distribution functions.. In order to determine design wave height for the design of breakwaters and to evaluate the storm surge to determine extreme water level conditions for the port facility at Nandgaon extreme wave analysis was performed by considering the data between the years 1981 and 2010 (Fig 2). The details of these studies and the result thereof are discussed in this paper. The comparison between three distribution functions applicability is also discussed.

Figure 1 Location Map of the Proposed site

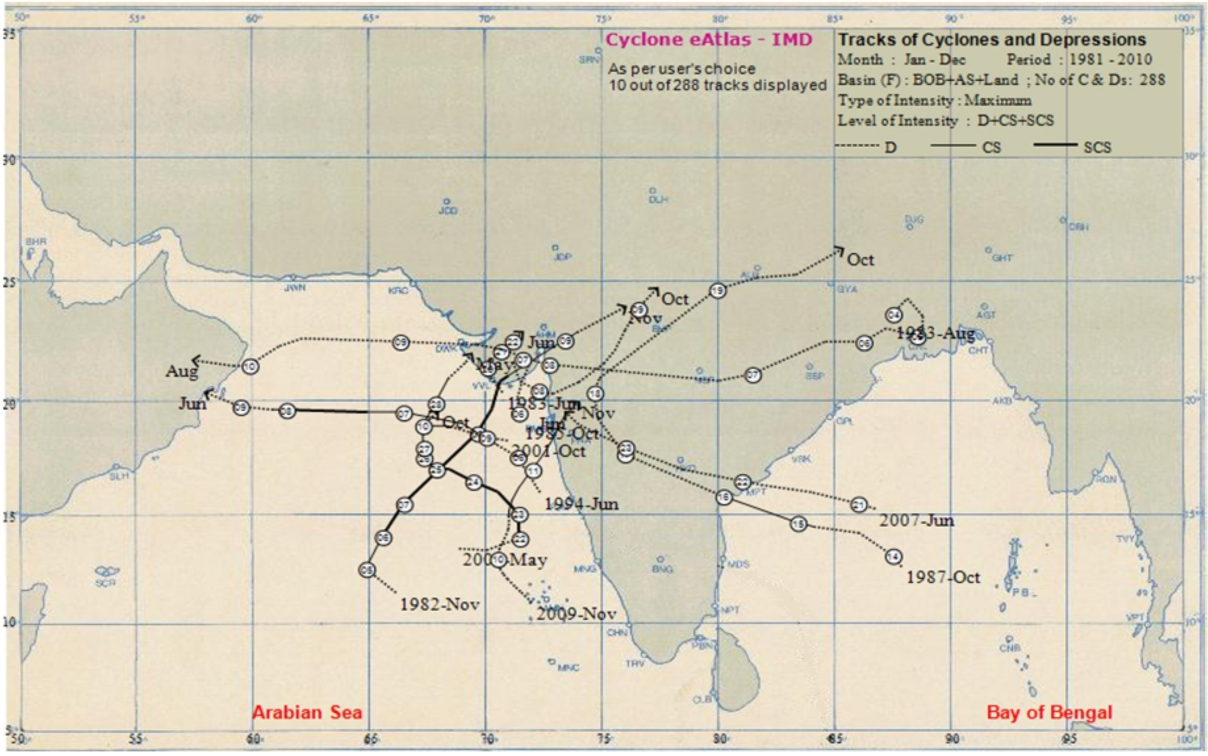

Figure 2 Storm crossing the land 100 km on either side of the Nandgaon

2.0 WAVE CLIMATE AND WAVE DATA

Wave climate refers to the general condition of sea state at a particular location. The parameters in wave climate are wave height, its period and direction. In random wave data analysis significant wave height (Hs) is usually considered as a height parameter. The other parameters are peak period (Tp) and Average period (Tz). The direction of wave is expressed in the form of wave rose diagram. The wave direction is expressed as sixteen point sector of bearing system i.e. ESE, SW, N etc. Ideally, the determination of extreme surge and water levels should be based on the statistical analysis of long-term measurements. Since the long-term measurements of storm surge and water levels , which occur during the storm (cyclonic) conditions, are seldom available, the extreme value analysis for the storm is carried out using hindcast storm data (predicted values using past storm data). The extreme value analysis of these hindcast data provides the storm surge and water levels of various return periods required for the design of coastal structures. The common wave data sources are visually observed data, Instrumental measured data and hindcast storm wave data.

2.1 Hindcast wave and storm surge data

Estimation of waves generated by the storms in the past is called 'Wave Hindcasting'. Wave hindcasting is generally used to obtain storm wave data for extreme value analysis, since the long-term measured data are seldom available. Storm surge is the temporary rise in the water level near the coastline during the cyclone. This temporary rise in the water level occurs only when the cyclonic wind blows over the continental shelf and pushes the water against the coastline. Ocean waves are generated by the wind blowing over the water surface. The parameters, which govern the wave and surge generation are :

1) Wind speed
2) Duration of wind
3) Distance over which the wind blows – Fetch
4) Distance between point of observation and front of fetch area – Decay distance
5) Isobaric pressure gradient
6) The width of the continental shelf
7) Water depth at the edge of the continental shelf
8) Water depth at the observation site

A combined empirical-analytical procedure was developed by Sverdrup and Munk, which was revised by Bretschneider, based on empirical data (Shore protection Manual 1984). This wave prediction system is called as the "Sverdrup-Munk-Bretschneider (SMB) Method". Using the SMB method for hindcasting of storm waves, the significant wave height (Hs) and the peak wave period (Tp) could be predicted for a particular site. The data regarding wind speed, wind duration, fetch length and decay distance is obtained from the storm tracks and the synoptic charts. The wind speed is determined from the pressure gradient and the latitude of the fetch area. The pressure gradient is determined from the isobar spacing shown on the synoptic chart.

3.0 ESTIMATION OF DESIGN WAVE CONDITION FOR NANDGAON SITE

From the storm data for the period between years 1981 and 2010 (30 years), the storms passing through the area in the close vicinity of Nandgaon coast were identified . It was seen that there were total 10 such storms which crossed the coastline within the 100 km radius of the Nandgaon during 1981 and 2010. However, considering the importance of the project and to use the values for return period analysis storms passing within 300 km periphery of Nandgaon have been considered for the studies. 49 storms which are significant to the Nandgaon coast are considered for the present studies (Fig 2).

The storms were analysed using SMB method of hindcasting. It is observed from the analysis of the storm data during 1981 to 2010 that 17 data sets generated wave heights (Hs) of the order of higher than 2.0 m . The Super cyclone of 4th June 2007 generated the highest waves with significant wave height (Hs) of 5.51 m in the water depth of 40 m.

3.1 Extreme Value Analysis of Storm Wave Data :

For the extreme value analysis the Gumbel, Weibull and Log-Normal distribution are applicable (Herbich J.B. 1990). As such results of the extreme wave data were fitted to Gumbel, Weibull and Log-Normal distributions functions. The plots of Gumbel, Weibull and Log-Normal distributions are shown in Figs.3, 4 & 5 respectively..

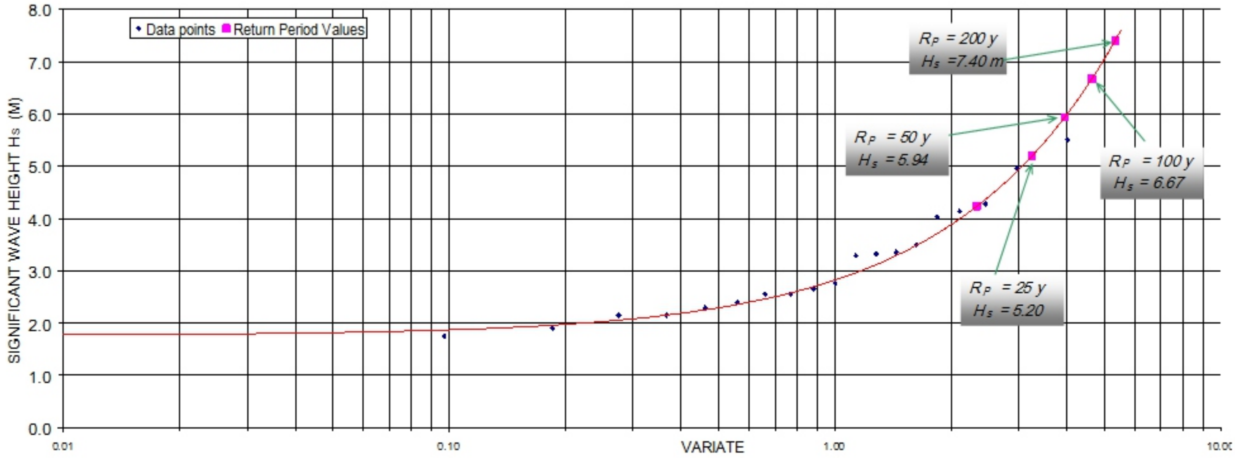

Figure 3 Hindcast storm wave data of Nadgaon site by Gumbel Distribution

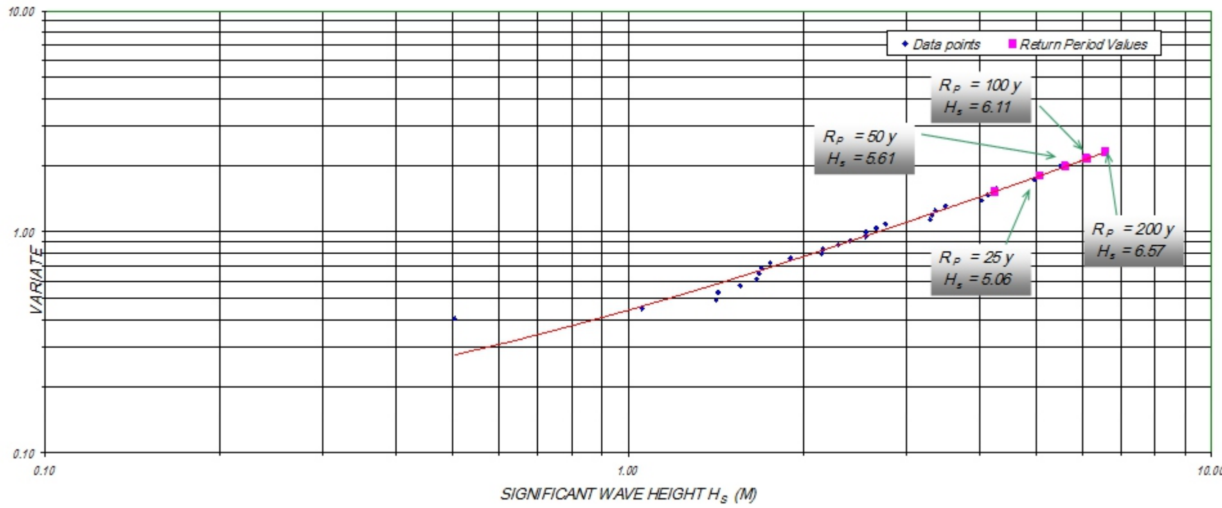

Figure 4 Hindcast storm wave data of Nadgaon site by Weibull Distribution

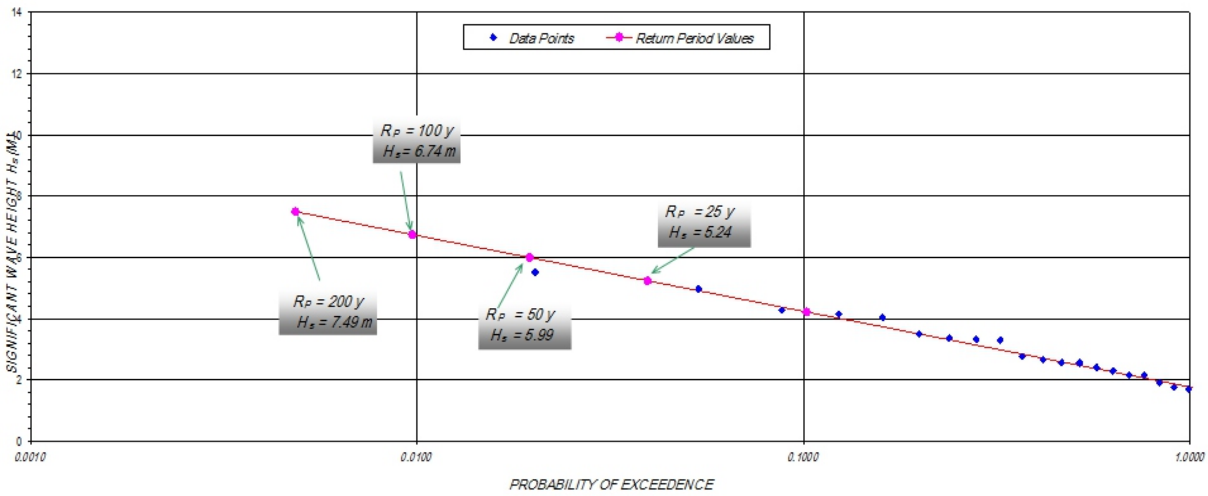

Figure 5 Hindcast storm wave data of Nandgaon site by Log-Normal Distribution

The estimates of extreme wave heights for different return periods using Gumbel, Weibull and Lognormal distributions are given in Table - 1. It is seen that the wave heights predicted using Gumbel, Weibull and Log-Normal distributions do not show much variation.

Table 1 Predicted Wave Heights off Nandgaon Coast (40 m Water Depth)

Return Period R_p in years	Predicted Significant Wave Height, H_s in metres		
	Gumbel	Weibull	Log-Normal
25	5.20	4.25	5.24
50	5.94	5.06	5.99
100	6.67	5.61	6.74
200	7.40	6.11	7.49

The average of these three values for each return period which would be more appropriate has been considered and shown in Table 2. The 200 - year return-period significant wave height of Nandgaon coast in a water depth of 40 m is predicted as 7.15 m.

Table 2 Predicted Extreme Wave Heights off Nandgaon Coast (40 m Water Depth)

Return Period R_p in years	**H_s in metres**
25	**5.17**
50	**5.85**
100	**6.51**
200	**7.15**

3.2 Estimation of Water Levels conditions for Nandgaon Site

3.2.1 Storm Surge Analysis :

Rise in the normal water level due to storms is called as "Storm Surge". The storm surge at or near the shoreline is due to two main components viz. (a) inverted barometric pressure effect and (b) onshore wind stress effect. The computations of the storm surge for the storms in the vicinity of port Nandgaon area for each of the above two components are described in the following paragraphs.

a) Inverted Barometric Effect :

The inverted barometric effect is the tendency for the water surface to be sucked upwards in regions of low atmospheric pressure. During the storm conditions, the water surface rise is centred at the eye of the storm and depends directly on the central pressure relative to normal sea-level pressure.
The surge due to inverted barometric effect (Sa) is given by (Silvester, 1974):

$$S_a = 0.01(P_n - P_0) \text{ in metres} \quad \text{..........} \quad (1)$$

Where,

Pn = Pressure of the isobar at the boundary of storm, in mb
Po = Pressure at the centre of storm, in mb

The central pressure (Po) is generally not mentioned on the synoptic charts. However, it can be computed using Hydromet-Rankin Vortex Model for the cyclones [Herbich,1990]. The pressure profile of a cyclone in Hydromet-Rankin Model is given by :

$$\frac{P_r - P_0}{P_n - P_0} = e^{-R/r} \quad \text{.....................} \quad (2)$$

Where,

r = Radial distance from the centre of storm in km
R = Radial distance of maximum cyclostrophic wind from the centre of storm in km
Pr = Pressure at radial distance 'r' in mb

The set of the values of Pr and r can be obtained from the synoptic chart and equation (4) can be solved for Po and R. A typical pressure profile for 04th June, 2007 cyclone is shown in Fig. 6.

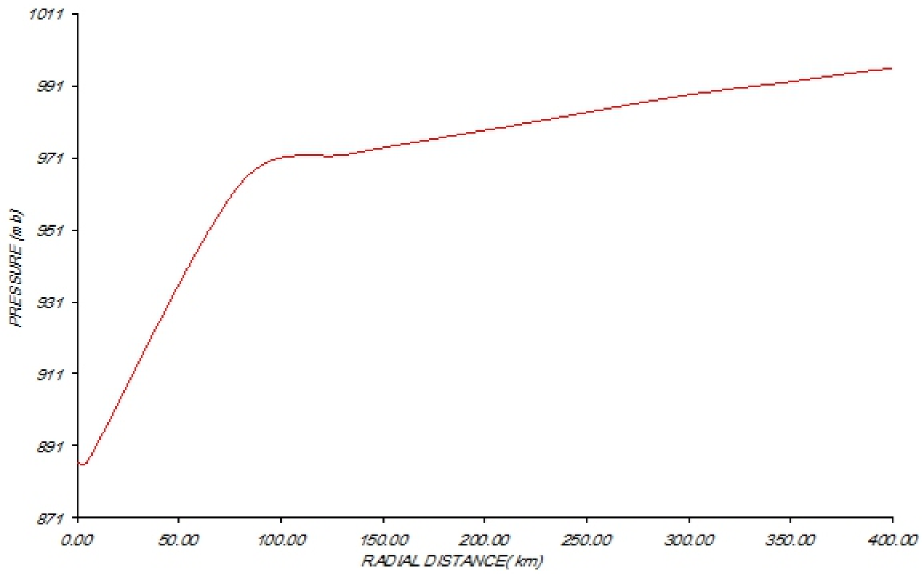

Figure 6 Pressure Distribution Curve for Storm on 04th June 2007 (0830 hrs)

b) Wind Stress Effect :

Generally, the larger component of any storm surge is that due to the wind stress on the water surface. The storm surge at the shoreline of an open ocean (i.e. storm surge over the continental shelf) due to static wind field is given by Silvester (1974) as :

$$S_w = \frac{kU^2 L}{g(d_1 - d_2 - S_w)} \ln\left(\frac{d_1}{d_2 + S_w}\right) \qquad \text{....................} \qquad (3)$$

Where,

Sw = Storm surge due to wind stress in meters

k = Wind stress co-efficient

= 0.000003 for open ocean,

= 0.0000033 for enclosed/semi enclosed water bodies

U = Surface wind speed in m/sec

L = Length or Fetch over which wind is blowing in meters. (Taken as width of the continental shelf if fetch is larger than the width of the continental shelf)

g = Acceleration due to gravity (9.81 m/sec2)

d1 = Depth of the water at the edge of the continental shelf in m

d2 = Depth of the water near the coast in meters

The above equation is for surge over the continental shelf. The profile of the continental shelf at the coast of port Nandgaon is shown in Fig. 7, which was plotted from the Hydrographic Chart - 21 The following values are taken for the water level computations from the Fig. 7 :

L = 282 km

d1 = 204.90 m

d2 = 4.90 m (at Mean High Water Spring)

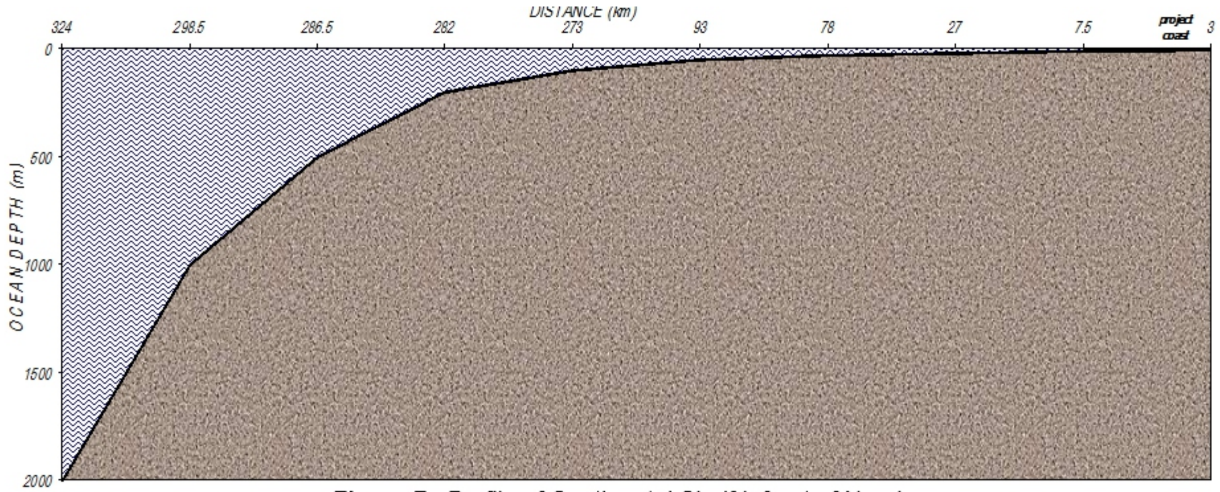

Figure 7 Profile of Continental Shelf Infront of Nandagaon
(Ref : Hydrographic Chart No.21)

3.2.2 Results of Storm Surge Analysis :

In the storm surge analysis, all the storms were assumed to occur in front of site on the continental shelf, since the storm surge gets generated only if the wind blows over the shallower depths of water i.e. on the continental shelf. The values of the storm surge due to inverted barometric effect (Sa) and due to wind stress (Sw) were computed for all the storms, which were significant for the port Nandgaon. Total storm surge 'S' was computed by adding these two components. Although these two components cannot occur simultaneously, the design storm surge is generally computed by adding these two components for all engineering purposes. There are 25 storm conditions, which generated a total storm surge of 0.50 m or higher at the port Nandgaon. There are 15 events which generated total storm surge of 1.0 m and above.

Besides the wind stress forcing the water shoreward, the reduction of atmospheric pressure at the centre of the storm also causes a rise in the water level, as mentioned earlier. The maximum barometric surge may be concurrent with the wind stress surge or it may precede or follow it. For engineering purposes, it is desirable to consider them as synchronous. Considering these two effects synchronous, the total surge at the Port Nandgaon during the severe cyclone of 4th June, 1977 works out as 3.38 m.

3.2.3 Extreme Value Analysis of Storm Surge Data:

Results of the extreme wave data fitted to Gumbel, Weibull and Log-Normal distributions functions are given in Table 3. The plots of Gumbel, Weibull and Log-Normal distributions are shown in Figs.8, 9 & 10 respectively.

Table 3 Predicted Storm Surge at Nandgaon Coast

Return Period Rp in years	Predicted Storm Surge (SS) in metres		
	Gumbel	Weibull	Log-Normal
25	2.32	2.31	2.25
50	2.65	2.67	2.54
100	2.99	3.02	2.82

It is seen that the storm surge predicted using Gumbel, Weibull and Lognormal distributions are almost similar. Average of these three values for each return period, which would be more appropriate for consideration is shwon in Table – 4.

Table 4 Predicted Extreme Storm Surge at port Nandgaon Coast

Return Period Rp in years	Storm Surge (SS) in metres
25	2.3
50	2.6
100	2.9

It is seen that the 100 – year, 50 - year and 25 – year storm surge for the Port Nandgaon is predicted as 2.9 m, 2.6 m and 2.3 m respectively. As such, this storm surge values may be considered in the estimation of extreme water level at the shore.

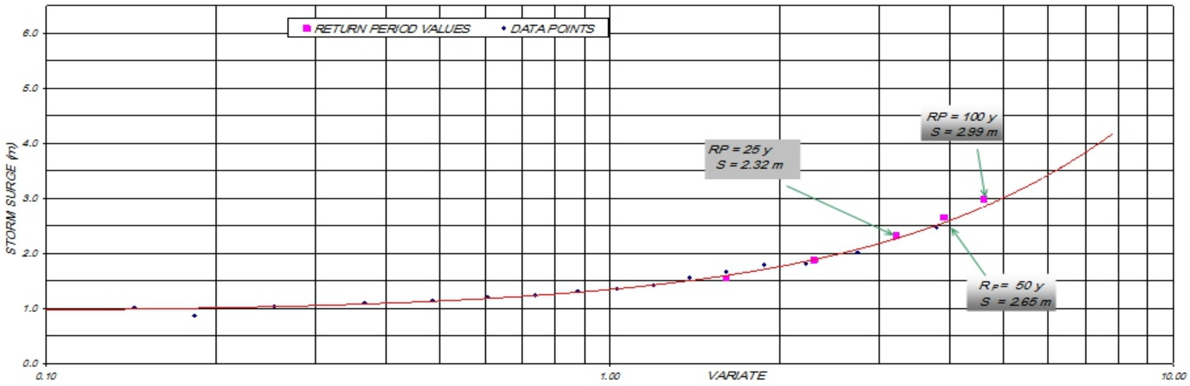

Figure 8 Hindcast storm Surge data of Nandgaon site by Gumbel Distribution

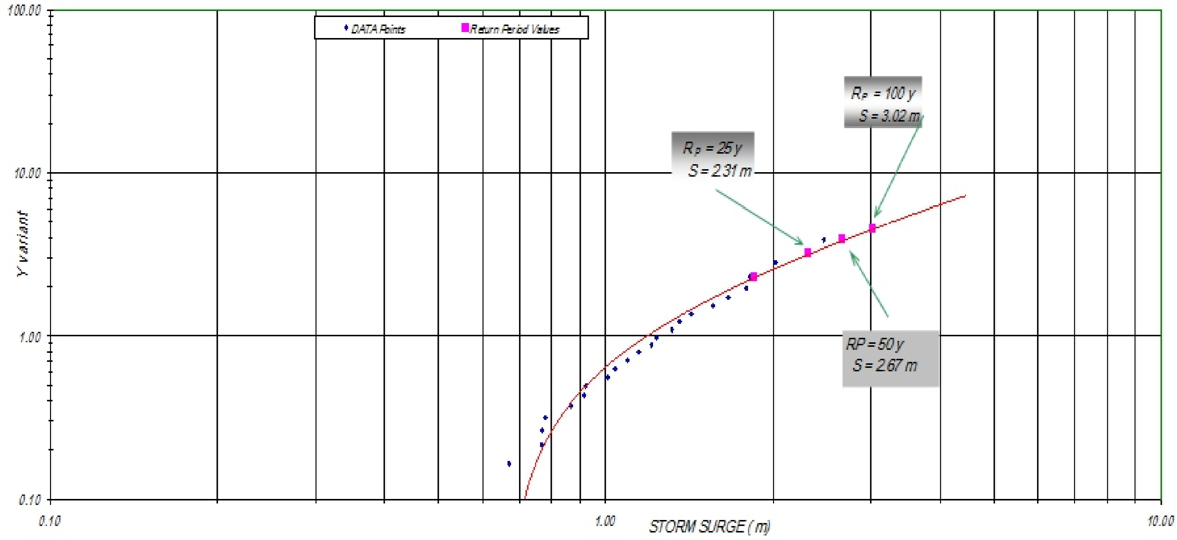

Figure 9 Hindcast storm Surge data of Nandgaon site by Weibull Distribution

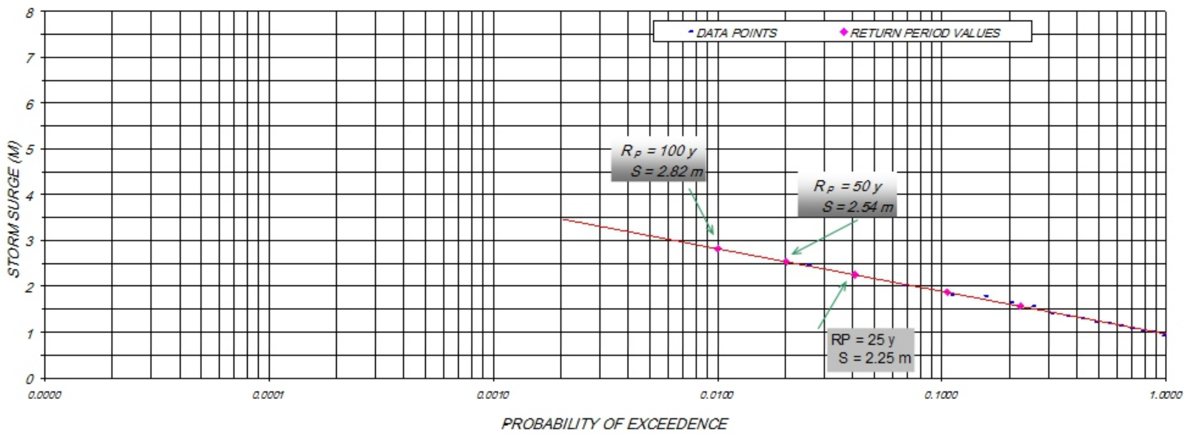

Figure 10 Hindcast storm Surge data of Nandgaon site by Log - Normal Distribution

4. CONCLUDING REMARKS

Based on the hindcasting studies carried out for water level and wave conditions using the storm data for Nandgaon site, the following conclusion are made:

- Storm wave hindcasting analysis indicated the design wave value of 7.1 m, 6.1 m, 5.8 m and 5.1 m for the return periods of 200 – year, 100 – year, 50 – year and 25 – year respectively.
- Storm surge analysis indicated the water level values of 2.9 m, 2.6 m, and 2.3 m for the return periods 100 – year, 50 – year and 25 – year return period respectively.
- These parameters would be useful to arrive the design wave and water level conditions for the proposed development of Port facility at Nandgaon.

REFERENCES

Herbich J.B. (1990), "Handbook of Coastal and Ocean Engineering, Vol. 1", Gulf Publishing Company, Houston, Texas.

Silvester R. (1974) "Coastal Engineering, Vol. II", Elsevier Scientific Publishing Company, Amsterdam, Netherlands.

Shore Protection Manual (1984), U.S. Army Engineering Waterways Experiments Station, Coastal and Hydraulics Laboratory, US Army Engineers R&D Centre, Vicksburg.

Bed Load Transport in the Presence of Different Concentrations of Wash Load

N K Khullar[1] , Sushma Walia[2], Nitin Samaiya[3],

[1]FIAH, Prof.-cum-Head, Department of Civil Engineering, PAU Ludhiana-141004
khulrdce@rediffmail.com
[2]MIAH2 Research Scholar, Department of Civil Engineering, TU Patiala-147004
sushmawalia@yahoo.com
[3]Assistant Professor, Department of Civil Engineering, JP University Guna, Madhya Pradesh
nitinsam@rediffmail.com

ABSTRACT

Many methods are available for the computation of bed load transport of uniform and non uniform sediments. The methods available for bed load transport have been developed using data on bed load transport in clear water flow. For the computation of bed load transport using these methods the sediment characteristics and the flow characteristics are required. The characteristics of sediment and flow may change in the presence of different concentration of fine sediments in the flow and as such may affect the bed load transport. In the present study statistical and graphical analyses are used to demonstrate the performance and variations of bed load transport rates for uniform and non-uniform sediments. Results of statistical analysis are used to compare bed load transport methods of Patel and Ranga Raju (1996, Karim (1998) and Wu et al (2000) between observed and computed bed load transport is used to identify the best method for computation of bed load transport in the presence of different concentration of wash load in the flow.

Keywords—Bed load, sediment characteristics, flow characteristics and wash load.

1. INTRODUCTION

Bedload is that portion of the total sediment in transport that is carried by intermittent contact with the streambed by rolling, sliding, and bouncing when the bed shear stress exceeds a critical value. The ability of any formula to predict the bed-load transport rate under given flow conditions is predicated on the assumption that it is possible to describe the rate at which bed load is transported in terms of measurable hydraulic and sediment data (Gomez B, 2006). A lot of wash load/fine sediment load comes to the streams/channels during rainy season due to erosion of soil from the catchment and affects bed composition (Khullar, 2003; Khullar et al., 2007 and Samaiya, 2009). The sediment in suspension may affect the flow turbulence and may also change the bed features (Khullar, 2003; Khullar et al., 2007). These fine suspended sediment particles dampen the turbulence or interfere with the production of turbulence near the bed where the concentration of these particles as well as the rate of turbulence production is maximum and as such will also affect resistance to flow and sediment transport. As a result the resistance to flow may increase or decrease.

1.1 Wash load

The wash load is comprised of moving sediment particles that are derived from upstream sources other than the channel bed. Wash load is not found in appreciable quantities in the stream bed. It is mostly finer in size than the sediment of bed material load and it is considered not to interact with bed material (Wu, 2007). Einstein et al (1940) defined wash load as the size fraction of total sediment load not present in significant amounts in the stream bed and banks and which is easily washed away by the flow. Einstein (1950) defined wash load as the grain size of which 10% of the bed material mixture is finer. It should be noted that the definition of wash load and bed-material load depends on flow and sediment conditions. According to Shen (1970) the wash load is that sediment size for which the sediment supply rate is less than the sediment transport capacity of a channel for the given hydraulic conditions. According to Woo et al (1987) the size limit for wash load cannot be stipulated. Wash load consists of very fine silt and clays, which have diameters smaller than 0.0625 mm (Garde and Ranga Raju, 2000). The wash load effect the fluid properties and settling velocity of the larger sediment particles. Recent studies carried out at Roorkee (Khullar; 2003, Khullar et al; 2010) and abroad (Yang et al, 2005) have questioned the general conception about the wash load transport and found that the wash load does have a functional relationship with the hydraulics of the flow. As per Khullar et al (2010) the wash load do interact with the coarse bed material during their transport. The proportions of wash load increases in the bed material with increase in concentration of wash load in the flow.

1.2 Effect of presence of wash load on bed load transport

The transport of bed material load is believed to be affected due to presence of wash load in the flow as the resistance to flow is affected due to its presence. Only a few studies have been carried out to understand the effect of wash load on transport of the bed material. However, the natural channel bed material consists of nonuniform bed material; the problems related to nonuniform sediment transport are extremely complex, especially when consideration is given to the shelter-exposure interactions of bed particles of different sizes.

Kikkawa and Fukuoka (1969) found that the rate of bed material transport increased with increase in wash load concentration. Wan (1985) observed sediment particles to settle more slowly in the presence of bentonite suspension as compared to clear water condition. Due to larger threshold velocity and smaller settling velocity, the bed load was found to be smaller and the suspended load to be larger than that in case of transport without wash load. Woo et al (1987) carried out study to test the applicability of existing sediment transport formulae namely Einstein's (1950) and Colby's (1964) for predicting the total bed sediment discharge in flows having clay suspensions. Woo et al (1987) used flume data of Simons et al (1963) having bed material size 0.47 mm to 0.54 mm, and found that the total transport rate of bed material was more than that given by the two methods mentioned above. This was due to decrease in settling velocity of suspended sediment particles in the presence of clay suspensions. Diplas and Parker (1992) found that when the amount of fines deposited in the bed was about 5 per cent of the sub-pavement material, the bed load transport started to decline. The observed reduction of bed load transport was upto 57 per cent in the presence of fines as compared to the corresponding transport in flow not transporting suspended load.

Khullar (2003) proposed new relationships for the computation of bed load transport and suspended load transport of uniform and non uniform sediments in the presence of different concentrations of cohesion less wash load in the flow. Similar investigations also need to be made using the cohesive wash load in the flow.

2. REVIEW OF LITERATURE

Patel and Ranga Raju (1996) proposed an empirical relationship for computing the bed load transport of uniform and non uniform sediment in clear water streams. According to them the dimensionless bed load transport rate is a function of dimensionless effective shear stress and exposure cum sheltering factor. Yang et al (1996) computed total bed material load in a sediment laden river with a high concentration of fine suspended materials using Yang's modified unit stream formula. Theoretical and laboratory studies indicate that modification can be made on the values of particle fall velocity, flow viscosity and relative specific weight without any change of the coefficients used in Yang's original formula. Comparisons between computed results from the modified unit stream formula and field indicate that the modified formula can be used to compute total bed material load with accuracy. Karim(1998) proposed the relation for predicting sediment transport for non uniform sediments in a clear water stream. According to him sediment transport rate is a function of flow velocity, fall velocity of sediment, shear velocity, proportion of sediments of a particular size o n the surface of bed, sediment size etc. He considered the interaction between different size fraction of sediment by introducing a sheltering factor reflecting reduction in the transport of finer particles by coarser particles and a factor reflecting the areal fraction of bed sediments.Sun and Donahue (2000) proposed a method for fractionwise bed load computation of non-uniform sediment using stochastic method of sediment fractional bed load transport rates. Wu et al (2000) proposed a method for fraction wise calculation of bed load transport using the hiding and exposure concept of sediment in the bed. They proposed a probabilistic model for predicting the hiding and exposure correction factor in case of non uniform sediments. It takes into account the influence of sediment size and the bed material gradation. Molinas and Baosheng (2000) compared different fractions of bed-material load using three different methods for nonuniform sediments and found that the discrepancy ratios between the computed and observed fractional bed load transport rates are smaller for size fractions close to median size of sediments and larger for fractions finer and coarser than the median size of sediment mixture. The methods used by them are the direct computation by size fraction approach, the bed material fraction (BMF) approach and the transport capacity fraction (TCF) approach. Statistical analysis and graphical comparison are utilized to demonstrate the performance and variations in different methods. According to them the method based on transport capacity approach provide reasonable predictions for bed load transport rate except Li (1998) data.

Wilcock *et al* (2001) conducted experiments with gravel and sand mixture being bed material and found that as the sand proportion was increased, the gravel transport rate was also increased even though the proportions of gravel in the bed decreased. They concluded that the methods of sediment transport and sorting and predictions of stream channel response to finer sediment inputs are required to be reinvestigated to account for the effect of fine particles concentration. Kleinhans and Van Rijn (2002) proposed a stochastic model to predict transport rates of a nonuniform sediment mixture. The hiding-exposure function was considered to be the main uncertainty in the prediction of transport rates for different size fractions. It is proposed to use an equal mobility approach for unimodal sediments and the function of Egiazaroff (1965) for bimodal sediments. According to Bravo-Espinosa *et al* (2003) bed load transport rates in alluvial channels are dependent on individual particle-size fractions rather than on the complete spectrum of particle sizes represented by one characteristic particle size. They described functional relations between particle-size fractions and stream power. Yang *et al* (2003) developed user-friendly total bed-material load transport formula based on dimensional analysis for flow in alluvial channels under equilibrium transport conditions. The main advantages of this formula are its ease of computation, accuracy in prediction, and the wide range of application. The total sediment discharge is computed directly and is linearly related to the new total load transport parameter, *TT*. The latter involves variables that can be easily measured in field conditions, i.e., flow depth, mean flow velocity, energy slope, median sediment size and density, and water temperature. The factor of proportionality k in the formula has been checked for a wide range of hydraulic conditions and it remains a constant equal to 12.5. Comparisons between the computed and measured total sediment discharge indicate that the predictions are good. Baosheng *et al (2004) proposed a size gradation correction factor* K_d to account for the log-normal distribution of non-uniform bed material. According to them the use of Kd in conjunction of bed material load equations originally developed for single particle sizes, improve the accuracy of transport calculations for sediment mixtures. This method is applicable to laboratory flumes and natural rivers with median diameter D50 of bed material in the sand size ranges. The improvement on transport rate by Kd factor is significant for data having σg greater than 2, while the correction is negligible for data with σg less than 1.5.

Yang (2005) proposed a relationship between flow strength and sediment discharge. He found that sediment transport rate in unidirectional flows can be well predicted when energy dissipation rate is defined as the product of total shear stress and near bed shear velocity related to grains. Sinnakaudan et al (2006) proposed new total bed material load equation that is applicable for rivers in Malaysia by using multiple linear regression analyses. A total of 346 hydraulic and sediment data were collected from nine natural and channelized rivers having diverse catchment characteristics in Malaysia. The governing parameters were carefully selected based on literature survey and field experiments, examined and grouped into five categories namely mobility, transport, sediment, shape, and flow resistance parameters. The most influential parameters from each group were selected by using all possible regression model method. The suitable model selection criteria namely the R-square, adjusted R-square, mean square error, and Mallow's Cp statistics were employed. The accuracy of the derived model is determined using the discrepancy ratio, which is a ratio of the calculated values to the measured values. The best performing models that give the highest percentage of prediction from the validation data were chosen. In general, the newly derived model is best suited for rivers with uniform sediment size distribution with a d50 value within the range of 0.37–4.0 mm and performs better than the commonly used Graf, Yang, and Ackers–White total bed material load equation. Khullar et al (2007b) found that bed load transport rate of uniform and nonuniform sediments are affected by presence of wash material in suspension. The wash material present in the flow effect the hydraulic parameter and as such their variation needs to be taken into account while computing the bed load transport. They proposed a new approach for computation of bed load transport in presence of different concentration of wash load in the flow. According to them the bed load can be computed by using Patel and Ranga Raju (1996) method provided the changes in hydraulic parameter due to presence of wash load in suspension are taken into account. Van Rijn (2007) discussed the properties of sediment beds over the full range of conditions (silts to gravel), in particular the effect of fine silt on the bed composition and on initiation of motion (critical conditions). High-quality bed-load transport data sets are identified and analyzed, showing that the bed-load transport in the sand range is related to velocity to power 2.5. The bed-load transport is not much affected by particle size. The prediction of bed roughness is addressed and the prediction of bed-load transport in steady river flow is extended to coastal flow applying an intra wave

Simplified bed-load transport formulas are presented, which can be used to obtain a quick estimate of bed-load transport in river and coastal flows. It is shown that the sediment transport of fine silts to coarse sand can be described in a unified model framework using fairly simple expressions. The proposed model is fully predictive in the sense that only the basic hydrodynamic parameters (depth, current velocity, wave height, wave period, etc.) and the basic sediment characteristics (d10, d50, d90, water temperature, and salinity) need to be known. The prediction of the effective bed roughness is an integral part of the model. Bathurst (2007) improved the relation for calculating bed load transport in mountain rivers under the condition when transport of coarser material occurred by breakup of the armor layer. He considered the at-a-site rate of change of bed load discharge with water discharge and relating this rate both to channel slope and to the degree of bed armoring. This latter dependency was introduced to account for the ease with which sediment is made available for transport as water discharge increases. Islam and Akhter (2007) predict that unit stream power formula and modified unit stream power formula are applicable for high concentration of fine sediments to estimate the sediment transport in the Gange River. The comparison between computed and observed sediment discharge based on Yang's formula and modified Yang's formula show that Yang's formula over predicts the sediment transport. The discrepancy ratio and standard deviation suggest that modified Yang's formula performs better for the sediment laden Gange River. The modified Yang's sediment transport function can be used in modeling sediment load in the Gange River. The Yang's formula can be used instead of the modified Yang's formula after adjusting the computed sediment load by an appropriate multiplying factor.

The review of literature indicates that the bed load transport is significantly affected by the presence of wash load. However, relationship for predicting bed load transport rates in the presence of wash load is not yet conclusive. The transport of bed material load has been studied a lot, but the effect of presence of wash load still requires further studies.

3. MATERIAL AND METHODS

Not many studies are available on bed load transport in the presence of wash load transport. Khullar (2003) performed experiments on bed load transport in a laboratory flume with bed having 1.8 mm uniform sediments, 0.96 mm uniform sediments and 2.1 mm sediment mixture as bed material in clear water flow and in sediment laden flow having 0.064 mm fine sediments in suspension. Different concentration of fine sediments were passed under the similar hydraulic condition i.e. discharge and slope as for clear water flow. Samaiya (2009) performed experiments on bed load transport in a laboratory flume with bed having 1.8 mm uniform sediments, 0.96 mm uniform sediments and 2.0 mm sediment mixture as bed material in clear water flow and in sediment laden flow having 0.0039 mm fine sediments in suspension. Different concentrations of fine sediments were passed under similar hydraulic condition, i.e. discharge and slope as for clear water flow. The experiments were performed in different series like 1UW series, 2UW series and MW series. Here 1U refers to the uniform sediment 1, 2U refers to the uniform sediment 2 and M refers to sediment mixture used by them. In each series different runs were taken by them by increasing the concentration of fine sediment in the flow. The first run in each series was taken with clear water flow. The bed load measurements were taken during all the runs of different series. Range of hydraulic data and bed load transport during these runs are given in Table 1.1 and the characteristics of bed material and fine sediment of the data used are given in Table 1.2.

Table 1.1 Range of hydraulic parameters used for bed load transport in presence of wash load

Data series	Q (m3/s)	h (m)	U (m/s)	Mk	S × 103	dw (mm)	s	qb ×103 (N/m-s)
Khullar(2002) (1UW Series)	0.0129- 0.0259	0.082 - 0.193	0.58 -0.82	0.806	1.79 - 3.82	0.064	2.65	2.25 - 735
Khullar(2002) (2UW Series)	0.0159 - 0.026	0.138 - 0.244	0.52 - 0.59	0.744	1.12 - 1.75	0.064	2.65	4.47-139
Khullar(2002) (MW Series)	0.0152- 0.0257	0.097 - 0.173	0.61 -0.81	0.31	2.44 - 3.74	0.064	2.65	3.5 - 225
Samaiya Study (1UW Series)	0.0176- 0.0286	0.143 - 0.201	0.57 -0.72	0.806	1.82 - 3.92	0.0039	2.65	26.593 - 158.489
Samaiya Study (2UW Series)	0.0094- 0.0235	0.096 - 0.224	0.46 -0.55	0.744	1.123 -3.71	0.0039	2.65	14.8 -269.2
Samaiya Study (MW Series)	0.0158- 0.0246	0.119 - 0.179	0.64 -0.73	0.3096	2.56 -3.746	0.0039	2.65	74.516 - 239.663

Table 1.2 Properties of the bed material and wash material

Sediment Designation	da (mm)	d50 (mm)	d65 (mm)	σg	Mk
Khullar 1U	1.794	1.8	1.9	1.15	0.806
Khullar 2U	1.03	0.96	1.2	1.3	0.744
Khullar M	2.73	2.1	3.15	2.25	0.31
Khullar W	-	0.064	-	-	-
Samaiya 1U	1.794	1.8	1.9	1.15	0.806
Samaiya 2U	1.03	0.96	1.2	1.3	0.744
Samaiya M	2.33	2	3.05	1.95	0.3096
Samaiya W	-	0.0039	-	-	-

3.1 Check on the existing methods for estimation of bed load transport rate

Many methods are available for the computation of bed load transport of uniform and non uniform sediments. The methods available for bed load transport have been developed using data on bed load transport in clear water flow. For the computation of bed load transport using these methods the sediment characteristics and the flow characteristics are required. As already discussed the characteristics of sediment and flow may change in the presence of different concentration of fine sediments in the flow and as such may affect the bed load transport.

Khullar et al (2007b) proposed the hypothesis that for the computation of bed load transport, the parameter of the original bed material should be used. The fines, if any, in the bed material should be ignored as they do not affect the exposure/ sheltering of coarse bed material. Using the hypothesis they have found that the method of Patel and Ranga Raju (1996) can be used to compute the bed load transport of uniform and non uniform sediment in the presence of different concentration of wash load provided the effect of change of resistance due to the presence of wash load is taken care of while computing bed load transport. Samaiya (2009) carried out experiment for bed load transport of uniform and non uniform sediment in the presence of different concentration of cohesive sediments of size 0.0039 mm in the flow.

In present study the methods proposed by Patel and Ranga Raju (1996), Karim (1998) and Wu *et al* (2000) have been used to compute the bed load transport in the presence of different concentration of wash load using the hypothesis of Khullar *et al* (2007b). The computed bed load transport is then compared with the observed bed load transport.

3.1.1 Patel and Ranga Raju method

Patel and Ranga Raju (1996) carried out extensive experiments on initiation of motion and bed load transport rates of different fractions of sediments mixtures. They checked the accuracy of different methods, viz. Egiazaroff (1965), Ashida and Michue (1971), Hayashi *et al* (1980), *Parker et al* (1982), Nakagawa and Tsujimoto (1980), Wiberg and Smith (1987) and Bridge and Bennet (1992). Using their own data and those from earlier studies covering a wide range of flow conditions and sediment non-uniformity, Patel and Ranga Raju (1996) proposed a new method for fraction-wise computation for bed load transport of uniform and non-uniform bed materials. They used composition of the bed material for the computation of sediment parameters. The functional relationship given by Patel and Ranga Raju (1996) is given as

$$\phi_{B,i} = \left(\frac{\tau_o^{'}}{\Delta\gamma_s d_i}, \xi_{B,i} \right) \quad (1)$$

Here $\xi_{B,i}$ is an exposure cum sheltering coefficient, di is the sediment size for the ith size fraction and $\phi_{B,i}$ is dimensionless bed load parameter and can be computed as

$$\phi_{B,i} = \frac{i_B q_B}{\gamma_s i_b} \sqrt{\frac{\gamma_w}{(\gamma_s - \gamma_w) g d_i^3}} \quad (2)$$

Here ib is the proportion of size fraction di in the bed material as obtained from sieve analysis, iB is the proportion of size fraction di in the bed load as obtained from sieve analysis and qB is the bed load transport by weight per unit width.

Patel and Ranga Raju (1996) proposed the following functional relationship for exposure and sheltering parameter $\xi_{B,i}$

$$\xi_{B,i} = f \left(\frac{\tau_o^{'}}{\Delta\gamma_s d_i}, \frac{\tau_o^{'}}{\tau_{oc}}, M_k \right) \quad (3)$$

Here τ_{oc} is the critical shear stress for arithmetic mean size da, of the sediment mixture as per Shields, and Mk is Kramer's coefficient and is defined as:

$$M_k = \frac{\sum_{0}^{50} d_i \Delta p_i}{\sum_{50}^{100} d_i \Delta p_i} \quad (4)$$

Here Δp_i is per cent of size di in bed material and is equal to the difference in per cent finer of bed material for size di and di+1.

In Eq. (3.21), τ_o' is given as:

$$\tau_o' = \gamma_w R_b' S \tag{5}$$

Here R_b' is the hydraulic radius corresponding to grain resistance and is given as

$$R_b' = (Un'/\sqrt{S})^{3/2} \tag{6}$$

Where n' is Manning's roughness coefficient corresponding to grains and can be computed as

$$n' = \frac{(d_{65})^{1/6}}{25.4} \text{ ,in SI units.} \tag{7}$$

Where, d65 is the particle size such that 65 per cent of the particles are finer than this size. Velocity of flow is calculated by Equation

$$U = \frac{q}{y} \tag{8}$$

Patel and Ranga Raju (1996) carried out detailed analysis of the data and taking the results of Misri et al (1984), Samaga et al (1986 a) and Mittal et al (1990) as guide, they found that

$$C_m \xi_{B,i} = 0.0713 \left(\frac{\tau_o'}{\Delta\gamma_s d_i} C_s \right)^{-0.75} \tag{9}$$

Here Cs is a parameter dependent on $\frac{\tau_o'}{\tau_{oc}}$ and Cm is a parameter dependent on Mk. The value of Cs can be computed as

$$\log(C_s) = -0.1957 - 0.9571\left[\log\frac{\tau_o'}{\tau_{oc}}\right] - 0.1949\left[\log\frac{\tau_o'}{\tau_{oc}}\right]^2 + 0.0644\left[\log\frac{\tau_o'}{\tau_{oc}}\right]^3 \tag{10}$$

The value of C_m is adopted as

$C_m = 1.0$ for Mk>0.38 (11a)

$C_m = 0.7092\log(M_k) + 1.293$ for 0.05 <Mk<0.38 (11b)

Khullar et al (2007b) reproduced the graphical relationship of Patel and Ranga Raju (1996) in the form of following equations to compute the dimensionless bed load transport rate $\Phi_{B,i}$ for different fractions of sediments in a non-uniform bed material for different values of $\left(\xi_{B,i}\frac{\tau_o'}{\Delta\gamma_s d_i}\right)$.

For $0.02 \le \left(\frac{\tau_o'}{\Delta\gamma_s d_i}, \xi_{B,i}\right) \le 0.062$

$$\phi_{B,i} = 10^8 \left(\frac{\tau_o'}{\Delta\gamma_s d_i}, \xi_{B,i}\right)^{8.345}$$

For $$0.062 \leq \left(\frac{\tau_o'}{\Delta\gamma_s d_i}, \xi_B \right) \leq 0.175$$

$$\phi_{B,i} = 2545.5\left(\frac{\tau_o'}{\Delta\gamma_s d_i}, \xi_{B,\,i} \right)^5 - 412.23\left(\frac{\tau_o'}{\Delta\gamma_s d_i}, \xi_{B,\,i} \right)^4$$

$$+\ 518.81\left(\frac{\tau_o'}{\Delta\gamma_s d_i}, \xi_{B,\,i} \right)^3 - 81.01\left(\frac{\tau_o'}{\Delta\gamma_s d_i}, \xi_{B,\,i} \right)^2$$

$$+\ 6.19\left(\frac{\tau_o'}{\Delta\gamma_s d_i}, \xi_{B,\,i} \right) - 0.178 \qquad (13)$$

For $$0.175 \leq \left(\frac{\tau_o'}{\Delta\gamma_s d_i}, \xi_{B,\,i} \right) \leq 1.83$$

For $$0.175 \leq \left(\frac{\tau_o'}{\Delta\gamma_s d_i}, \xi_{B,\,i} \right) \leq 1.83$$

$$\phi_{B,i} = 13.895\left(\frac{\tau_o'}{\Delta\gamma_s d_i}, \xi_{B,\,i} \right)^{1.9356} \qquad (14)$$

Following the method proposed by Patel and Ranga Raju (1996) $\left(\xi_{B,\,i} \frac{\tau_o'}{\Delta\gamma_s d_i} \right)$ can be computed and using Equations (12) to (14) $\Phi_{B,i}$ can be computed. Thus, using these $\Phi_{B,i}$ values bed load transport rates q_B can be calculated and compared with the observed bed load transport rates q_B.

3.1.2 Wu et al method

Wu et al (2000) proposed a probabilistic model to determine the hiding and exposure correction factor in transport of nonuniform sediments. The model takes into account the effect of sediment size and the bed material gradation. The non dimensional fractional bed load transport rate $\phi_{b,\,i}$ can be determined by the following relation:

$$\phi_{b,\,i} = 0.0053\left(\frac{\tau_0'}{\tau_{c,\,i}} - 1 \right)^{2.2} \qquad (15)$$

Here $\phi_{b,i}$ is also defined as

$$\phi_{b,i} = \frac{q_{b,i}}{\gamma_s p_{b,i}} \sqrt{\frac{\gamma_w}{(\gamma_s - \gamma_w) g d_i^3}} \tag{16}$$

where, $p_{b,i}$ is the per cent of ith fraction in the mixture, $\tau_0^{'}$ is grain shear stress and $\tau_{c,i}$ is the critical shear stress for size di in nonunifom sediment mixture and given as:

$$\tau_{c,i} = (\gamma_s - \gamma_w) d_i \tau_{*c} \left(\frac{p_{e,i}}{p_{h,i}} \right)^m \tag{17}$$

Where τ_{*c} is dimensionless critical shear stress for the mean size of the bed material and is taken as 0.03, m is an exponent and its value is - 0.6, $p_{h,i}$ and $p_{e,i}$ are the total hidden and exposed probabilities respectively for the sediment size di and are given as:

Where τ_{*c} is dimensionless critical shear stress for the mean size of the bed material and is taken as 0.03, m is an exponent and its value is - 0.6, $p_{h,i}$ and $p_{e,i}$ are the total hidden and exposed probabilities respectively for the sediment size di and are given as:

$$p_{h,i} = \sum_{j=1}^{N} p_{b,j} \frac{d_j}{d_i + d_j} \tag{18a}$$

$$p_{e,i} = \sum_{j=1}^{N} p_{b,j} \frac{d_i}{d_i + d_j} \tag{18b}$$

Where, $p_{b,j}$ is the percentage of jth fraction of the mixture, dj is particle size of jth fraction.

3.1.3 Karim method

Karim (1998) emphasized the interaction between different size fractions of sediment by introducing a sheltering factor reflecting reduction in the transport of finer particles by shelter from the coarser particles and a factor reflecting the areal fraction of bed sediments. He proposed following relationship

$$q_{b,i} = 0.00139 \sqrt{g d_i^3 \left(\frac{\rho_s - \rho_w}{\rho_w} \right)} \left(\frac{U}{\sqrt{g d_i \left(\frac{\rho_s - \rho_w}{\rho_w} \right)}} \right)^{2.7} \left(\frac{u_*}{\omega_i} \right)^{1.47} P_{a,i}\, \eta \tag{19}$$

Here, $q_{b,i}$ is the volumetric sediment discharge per unit width of the ith size fraction of bed load, ω_i is fall velocity for ith sediment size di, $P_{a,i}$ is the fraction of surface area covered by particles of ith size fraction and given as

$$P_{a,i} = \frac{P_i / d_i}{\sum_{i=1}^{i=N} P_i / d_i} \tag{20}$$

Here N is the total number of size fractions in a nonuniform sediment mixture and Pi volumetric fraction of sediment in an unit volume of bed material and η is the sheltering coefficient and given as

$$\eta = C_1 (d_i / d_{50})^{C_2} \tag{21}$$

Here $C_1 = 1.15(\omega_{50} / u_*)$ is a coefficient and $C_2 = 0.6(\omega_{50} / u_*)$ is an exponent. In case of uniform sediments $P_{a,i}$ η is taken as one.

3.2 Comparison of computed bed load transport results

Statistical and graphical analyses are used to demonstrate the performance and variations of bed load transport rates for uniform and non-uniform sediments. Results of statistical analysis are used to compare bed load transport methods of Patel and Ranga Raju (1996, Karim (1998) and Wu et al (2000). Five different statistical parameters as discussed below are adopted to indicate the goodness of fit of these methods.

Discrepancy ratio, Ri : The ratio of computed bed load to its corresponding observed value is defined as discrepancy ratio.

$$\text{Where } R_i = \frac{q_{B(\text{Computed})}}{q_{B(\text{Observed})}} \tag{22}$$

For a perfect fit, R_i= 1.

Average discrepancy ratio, R_{av} : It is the arithmetic average of discrepancy ratio and is computed as

$$R_{av} = \frac{\sum R_i}{n} \tag{23}$$

Standard Deviation (Sigma), σ : It is standard deviation of the discrepancy ratio and is computed as

$$\text{Where } \sigma = \frac{(R_i - R_{av})^2}{n} \tag{24}$$

For a perfect fit, σ =0

Mean normalized error (MNE) : It is a measure of mean normalized error of the observed value from the computed values. It is expressed as,

$$\text{MNE} = \frac{100}{\text{JN}} \sum_{j=1}^{J} \sum_{J=1}^{N_j} \left| \frac{q_{B(\text{computed})} - q_{B\,(\text{observed})}}{q_{B\,(\text{observed})}} \right| \tag{25}$$

In which j = data set number, j = 1,2,.., J; J = total number of data sets; N_i = number of points in a given data set; and JN = the total number of data points. For a perfect fit, MNE =0

The correlation coefficient, r : The correlation coefficient is a measure of how well trends in the computed values follow trends in the actual observed values. It is expressed as,

$$r = \frac{\sum_{j=1}^{J} \sum_{1=1}^{N_j} (q_{B\,(\text{computed})} - \bar{q}_{B\,(\text{computed})})(q_{B\,(\text{observed})} - \bar{q}_{B(\text{observed})})}{\sqrt{\sum_{j=1}^{J} \sum_{1=1}^{N_j} (q_{B\,(\text{computed})} - \bar{q}_{B\,(\text{computed})})^2 \sum_{j=1}^{J} \sum_{1=1}^{N_j} (q_{B(\text{observed})} - \bar{q}_{B(\text{observed})})^2}} \tag{26}$$

For perfect fit the coefficient of correlation is 1. The higher the value of coefficient of correlation, the better is the method.

Graphs are also plotted between observed and computed bed load transport for each of the above methods. The statistical analysis and the graphs between observed and computed bed load transport is then used to identify the best method for computation of bed load transport in the presence of different concentration of wash load in the flow.

3.3 Computation for bed load transport in the presence of wash load

The range of data regarding bed load transport rates of uniform and non-uniform sediments in the presence of wash load in the flow is used in present study as shown in Table 1.1. Recently developed methods of Patel and Ranga Raju (1996), Karim (1998) and Wu et al (2000) are used to compute the bed load transport in the presence of different concentration of wash load in the flow using the hypothesis of Khullar et al (2007). By using these methods the total bed load transport is computed. The statistical parameter like standard error, correlation co-efficient (r), average discrepancy ratio, standard deviation and mean normalized error are computed for each of these methods for total bed load transport.

3.3.1 Patel and Ranga Raju (1996) method

The bed load transport was computed for the uniform and non-uniform sediments for the data of Khullar (2003) and Samaiya (2009) under different concentration of wash load in the flow. The computations were done as per the procedure given under 3.1.1. The computed bed load transport is compared with the observed bed load transport. Fig. 1.1 shows the variation of total computed bed load transport and observed bed load transport by Patel and Ranga Raju (1996) method. Fig.1.1 shows that there is scatter of data on both sides of best fit line i.e. 1:1 slope line. The statistical analysis was carried out to find different statistical parameters like standard error, correlation co-efficient (r), average discrepancy ratio, standard deviation and mean normalized error as per procedure discussed under 3.2. The statistical analysis indicate that the average discrepancy ratio for the data is 1.89, the mean normalized error is 1.15, standard deviation is 2.54 and correlation co-efficient is 0.786. As per these parameters there is a good correlation between the observed and computed bed load transport by this method. 38.1 percent of data lies within discrepancy ratio of 0.75 to 1.25, 59.4 percent of data lies within discrepancy ratio of 0.5 to 1.5 and 78.7 percent of the data lies between discrepancy ratios 0.25 to 1.75

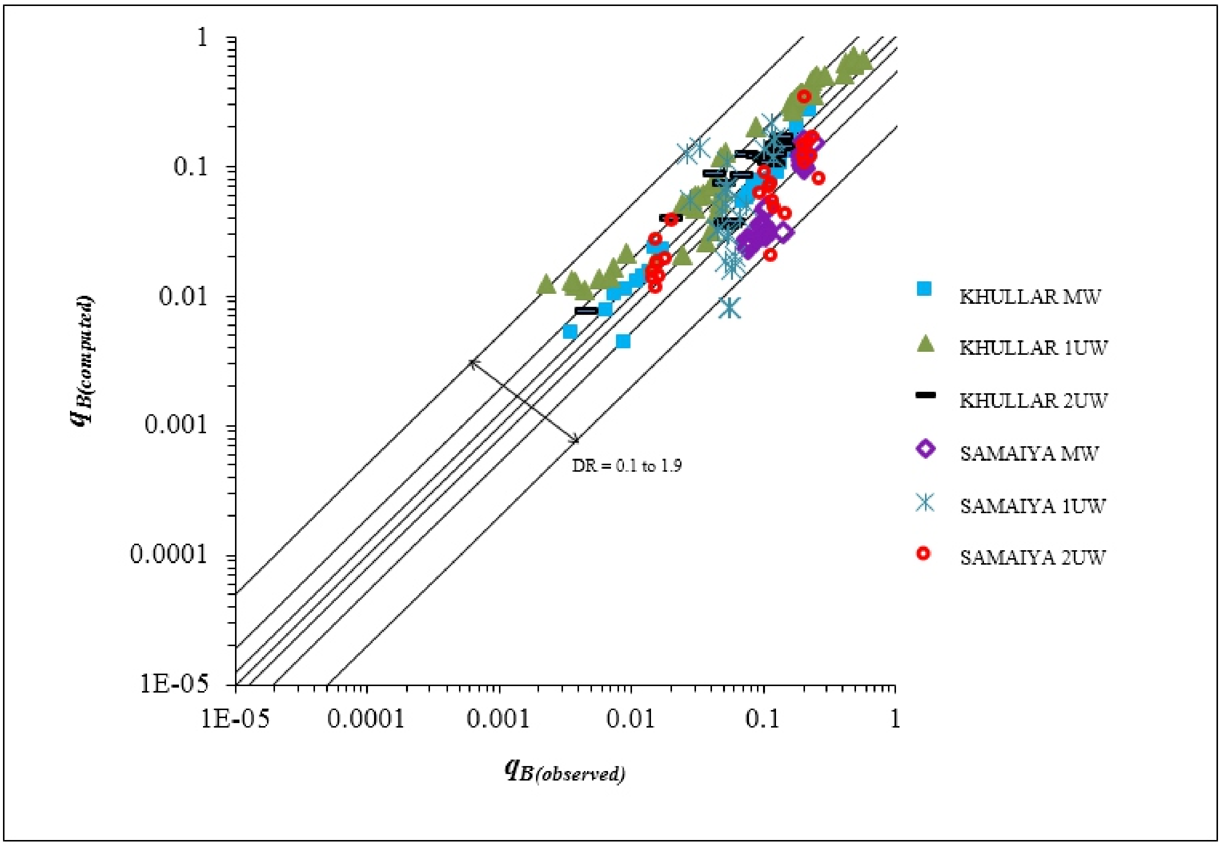

Fig1.1 Variation of bed load transport by Patel and Ranga Raju (1996)

3.3.2 Karim method (1998)

The bed load transport was computed for the uniform and non-uniform sediments for the Khullar (2003) and Samaiya (2009) under different concentration of wash load in the flow. The computations were done as per the procedure given under 3.1.3. The computed bed load transport is then compared with the observed bed load transport. Fig. 1.2 shows the variation of total computed bed load transport and observed bed load transport by Karim (1998) method. The statistical analysis was carried out to find different statistical parameters like standard error, correlation co-efficient (r), average discrepancy ratio, standard deviation and mean normalized error done as per the procedure discussed under 3.2. The statistical analysis indicate that the average discrepancy ratio for the data is 6.236, the mean normalized error is 5.1, standard deviation is 14.32 and correlation co-efficient is 0.11. As per these parameters there is poor correlation between the observed and computed bed load transport by this method. Fig. 1.2 also shows that the method of Karim (1998) generally over predicts the bed load transport. Table 4.1 further indicates that 9.6 percent of data lies within discrepancy ratio of 0.75 to 1.25, 16.7 percent of data lies within discrepancy ratio of 0.5 to 1.5 and 51.5 percent of the data lies between discrepancy ratios 0.25 to 1.75.

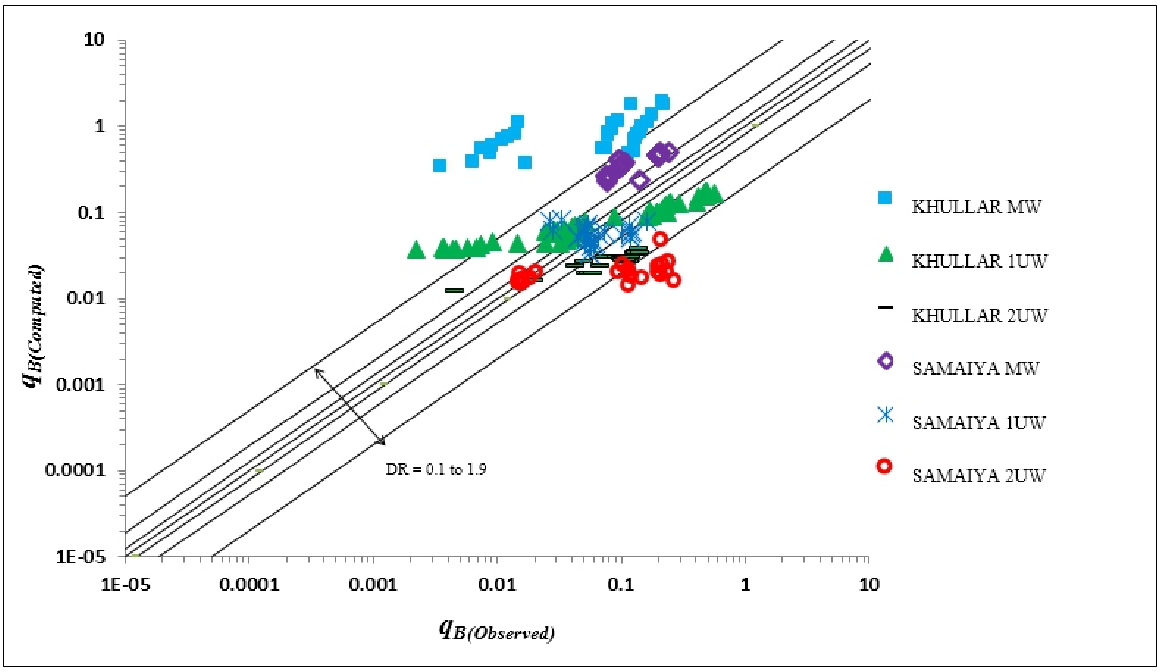

Fig. 1.2 Variation of bed load transport by Karim (1998)

3.3.3 Wu et al (2000) method

The bed load transport was computed for the uniform and non-uniform sediments for the data of Khullar (2003) and Samaiya (2009) under different concentration of wash load in the flow. The computations were done as per the procedure given under 3.1.2. The computed bed load transport is compared with the observed bed load transport. Fig. 1.3 shows the variation of total computed bed load transport and observed bed load transport by Wu et al (2000) method. The statistical analysis was carried out to find different statistical parameters like standard error, correlation co-efficient (r), average discrepancy ratio, standard deviation and mean normalized error as per procedure discussed under 3.2. The statistical analysis indicate that the average discrepancy ratio for the data is 1.38, the mean normalized error is 1.40, standard deviation is 2.77 and correlation co-efficient is 0.155. As per these parameters there is poor correlation between the observed and computed bed load transport by this method. Fig. 1.5 also shows that the method of Wu et al (2000) generally under predicts the bed load transport for most of the data. Table 4.1 further indicates that 5.1 percent of data lies within discrepancy ratio of 0.75 to 1.25, 14.14 percent of data lies within discrepancy ratio of 0.5 to 1.5 and 29.79 percent of the data lies between discrepancy ratios 0.25 to 1.75.

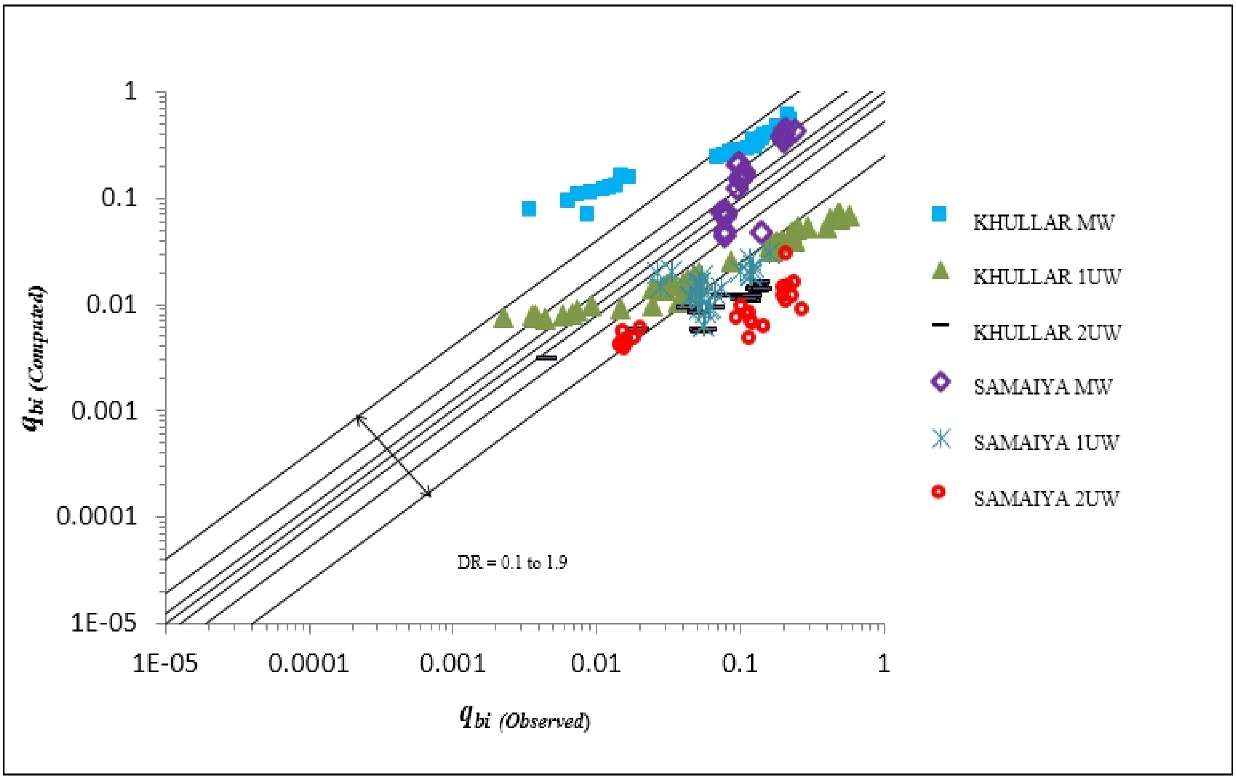

Fig. 1.3 Variation of bed load transport by Wu et al (2000)

Table 1.3 Comparison between computed and observed bed load transport rate by different methods

METHOD	DATA SOURCE	MNE	MEAN	DISCREPANCY RATIO (DR)						NO. OF POINTS
						PERCENT OF DATA IN				
				S.D	R	1.25-0.75	1.5-0.5	1.75-0.25	0.1–1.9	
PATEL AND RANGA RAJU (1996)	MW KHULLAR	0.234	0.998	0.272	0.946	65.52	93.1	100	100	29
	1U KHULLAR	2.19	3.18	3.43	0.977	32.31	50.77	63.08	64.62	65
	2U KHULLAR	0.299	1.07	0.61	0.893	50	73.08	96.15	100	26
	MW SAMAIYA	0.577	0.423	0.13	0.954	4	28	96	100	25
	1U SAMAIYA	0.584	1.28	0.78	0.859	35.71	60.71	71.43	75	28
	2U SAMAIYA	1.66	2.56	6.59	0.863	44	56	64	64	25
	TOTAL DATA RANGE	1.15	1.89	2.54	0.786	38.07	59.39	78.68	80.71	198
KARIM (1998)	MW KHULLAR	25.36	26.36	27.45	0.673	0	0	0	0	29
	1U KHULLAR	2.63	2.97	5.02	0.84	3.077	7.69	66.15	67.69	65
	2U KHULLAR	0.82	0.54	0.22	0.81	0	7.69	88.46	96.15	26
	MW SAMAIYA	2.06	3.06	0.709	0.821	0	0	4	4	25
	1U SAMAIYA	0.31	1.06	0.99	0.51	60.71	85.71	89.28	89.28	28
	2U SAMAIYA	0.75	0.74	0.72	0.346	0	8	40	96	25
	TOTAL DATA RANGE	5.11	6.236	14.32	0.11	9.595	16.66	51.52	60.1	198
WU	MW KHULLAR	4.92	5.92	4.91	0.98	0	0	0	0	29
ET AL (2000)	1U KHULLAR	0.89	0.71	1.1	0.939	9.231	18.46	32.31	87.69	65
	2U KHULLAR	0.873	0.1826	0.308	0.87	0	0	3.85	80.77	26
	MW SAMAIYA	0.629	1.49	0.521	0.93	16	32	64	76	25
	1U SAMAIYA	0.727	0.273	0.11	0.84	0	7.14	42.86	100	28
	2U SAMAIYA	0.75	0.2499	0.208	0.89	0	24	36	86	25
	TOTAL DATA RANGE	1.4	1.38	2.77	0.155	5.051	14.14	29.79	71.72	198

4. CONCLUSION

Comparison between the methods of Patel and Ranga Raju (1996), Karim (1998) and Wu et al (2000) for the computation of bed load transport in the presence of different concentration of wash load transport is made in Table 1.3 in terms of means normalize error and discrepancy ratio. Tables 1.3 indicate that 80.71 percent of the computed bed load transport by Patel and Ranga Raju (1996) lies between 0.1 to 1.9 discrepancy ratio. For the method of Karim (1998) this percentage is 60.10 and for Wu et al it is 71.72 percent. The comparison shows that overall the method of Patel and Ranga Raju (1996) is the best method for computation of bed load transport in the presence of different concentration of wash load in the flow.

REFERENCES

Bathurst J C (2007) Effect of course surface layer of bed load transport. J Hydraul Eng ASCE 133(11): 1192-1205.
Bravo-Espinosa M and Lopes V L (2003) Bedload transport in alluvial channels. J Hydraul Eng ASCE 129(10):783-95.
Bridge J S and Bennet S J (1992) A model for the entrainment of transport of sediment grains of mixed sizes, shapes and densities. Water Resour Res 28(2): 337-63.
Egiazaroff I V (1965) Calculation of non uniform sediment concentration. J Hydraul Eng ASCE 91(4):225-47.
Einstein H A, Anderson A G, and Johnson J W (1940) Distinction between bed load and suspended load in natural streams. Trans Am Geophys Union 21(2): 628-33.
Einstein H A (1950) The bed load function for sediment transportation in open channel flows. United States Dept of Agric Tech Bulletin No 1026: 1-71.
Garde R J and Ranga Raju K G (2000) Mechanics of sediment transportation and alluvial stream problems. Third Edition New Age International Publisher New Delhi, India 141-270.
Gomez B (2003) The potential rate of bed-load transport. Environmental Sciences, Geology. Proc Natl Acad Sci U S A.; 103(46): 17170–17173
Hayashi T Ozaki S and Ichibashi T (1980) Study on bed load transport of sediment mixtures. Proc 24th Japanese Conf Hydraulics 35-43.
Islam G M and Akhter S (2005) Sediment transport predictor in the Ganges River. J Civil Eng IEB 33(2): 65-74.
Karim F (1998) Bed material discharge prediction for non uniform bed sediments. J Hydraul Eng ASCE 124(4): 597-604.
Khullar N K (2003) Effect of wash load on transport of uniform and non uniform sediments. Ph.D. Thesis, Department of Civil Engineering, Indian Inst of Technology Roorkee, Roorkee, India.
Khullar N K, Kothyari U C and Ranga Raju K G (2007) Bed load transport in the presence of wash load transport. J Hydraul Res ISH 13(1): 106-22.
Khullar N K and Kothyari U C (2010) Study of bed features and Manning's roughness coefficient in laboratory flume in the presence of wash load. Proc of HYDRO 2010 held at Mullana University, Mullana, Ambala.
Kikkawa H and Fukuoka S (1969) The characteristics of flow with wash load. Proc13th Congr IAHR 2:233-240.
Kleinhans M G and Van Rijn L C (2002) Stochastic prediction of sediment transport in sand-gravel bed rivers. J Hydraul Eng ASCE 128(4): 412-25.
Molinas A and Wu B (1998) Effect of size gradation on transport of sediment mixtures. J HydraulEng ASCE 124(8): 786-93.
Molinas A and Wu B (2000) Comparison of fractional bed-material load computation methods in sand-bed channels. Earth Surf Process Landforms 25: 1045-68.
Nakagawa H and Tsujimoto T (1980) Sand bed inst ability due to bed load motion. J Hydraul Division ASCE 106(12): 2029-51.
Parker G Klingeman P C and Mclean D G (1982) Bed load and size distribution in paved gravel streams J Hydraul Eng ASCE 108(4): 544-71.
Samaiya N K and Kothyari U C (2007) Infiltration of cohesive wash material and bed material transport in an alluvial channel. J Hydraul Eng ISH 12(3):1-11.
Samaiya N K (2009) Effect of cohesive wash load on transport of non-uniform sediments. Ph.D Thesis Department of Civil Engineering, Indian Inst of Technology Roorkee, Roorkee, India.
Shen H W (1970) Wash load and bed load River Mechanics. Ed and Published by H W Shen, Fort Collins, Colarado 1: 11-30.
Sinnakaudan S K, AbGhani A, Ahmad M S S, and Zakaria N A (2006) Multiple linear regression model for total bed material load prediction. J Hydraul Eng ASCE 132(5): 521-528.
Simons D B Richardson E V and Haushid W L (1963) Some effects of fine sediments on flow phenomenon. Water Supply Paper No 1498G United States Geological Survey Washington D. C. USA.
Sun Z and Donahue J (2000) Statistically derived bed load formula for any fraction of nonuniform sediment. J Hydraul Eng ASCE 126(2): 105-111.
Wan Z (1985) Bed material movement in hyperconcentrated flows. J Hydraul Eng ASCE 111(6): 987-1001.
Wiberg P L and Smith J D (1987) Calculations of the critical shear stress for motion of uniform and heterogeneous sediments. Water Resour Res 23(8): 1471-80.
Wilcock P L, Kenworthy S T and Crowe J C (2001) Experimental study of the transport of mixed sand and gravel. Water Resources Research 37(12): 3349-58.
Wong M and Parker G (2006) Re-analysis and correction of bedload relation of Meyer-Peter and Muller using their own database. J Hydraul Eng ASCE 132(11): 1159–68.
Wu B and Molinas A (2000) Comparison of fractional bed-material load computation methods in sand-bed channels. Earth Surf Process Landforms 25: 1045-68.
Wiberg P L and Smith J D (1987) Calculations of the critical shear stress for motion of uniform and heterogeneous sediments. Water Resour Res 23(8): 1471-80.
Wilcock P L, Kenworthy S T and Crowe J C (2001) Experimental study of the transport of mixed sand and gravel. Water Resources Research 37(12): 3349-58.
Wong M and Parker G (2006) Re-analysis and correction of bedload relation of Meyer-Peter and Muller using their own database. J Hydraul Eng ASCE 132(11): 1159–68.
Wu B and Molinas A (2000) Comparison of fractional bed-material load computation methods in sand-bed channels. Earth Surf Process Landforms 25: 1045-68.
Wu B Molinas A and Julien P Y (2004) Bed material load computations for nonuniform sediments. J Hydraul Eng ASCE 130(10): 1002-12.
Yang C T, Molinas A and Wu B (1996) Sediment transport in the yellow river. J Hydraul Eng ASCE 122(5): 237-44.
Yang S, Qand Lim S (2003) Total Load Transport Formula for Flow in Alluvial Channels. J Hydraul Eng ASCE 129(1): 68–72.
Yang S Q (2005) Formula for sediment transport in rivers estuaries and coastal waters. J Hydraul Eng ASCE 131(11): 968-79.

Design of Branched Pipe Networks using Reliability and Total Annual Cost

Arkaja[1], Dr. P. S. Mahar[2], Dr. R. P. Singh[3],

[1]Ex M Tech student, Civil Engg.Deptt., College of Technology, GBPUA&T Pantnagar, 263145, Distt. Udham Singh Nagar (Uttarakhand), India Email: arkajakandari@gmail.com

[2]Professor, Civil Engineering Department , College of Technology, GBPUA&T Pantnagar, 263145, Distt. Udham Singh Nagar (Uttarakhand), India Email:pooransmahar@yahoo.co.in

[3]Professor, Irrigation & Drainage Engineering Department, College of Technology, GBPUA&T Pantnagar, 263145, Distt. Udham Singh Nagar (Uttarakhand), India Email:rajprasin1@rediffmail.com

ABSTRACT

The branched and looped type networks are the two basic configurations of water distribution. The branched pipe networks are generally designed by traditional and optimization methods. In the traditional method a pipe line is designed by balancing the available energy against the loss of energy due to friction whereas in the optimization methods the cost is minimized. For ensuring regular water supply it is important to consider the reliability of the water distribution network which depends on the failure rate of pipes, quality and quantity of water available at source and pressure requirements at demand nodes. Therefore the reliability of the system needs to be incorporated while minimizing the total cost of the distribution system. In this paper an enumerative method using both the reliability and total annual cost is developed for designing the branched pipe networks. The method satisfies the requirements of pressure and discharge along with the recommended values of the minimum and maximum velocities in the pipes. In this method different sets of pipe sizes are taken to calculate the reliability and cost of network and that set of pipe network is selected which has highest ratio of reliability to cost. To calculate the ratio of reliability to cost, the capital cost or the total annual cost can be used. The total annual cost is the sum of the annual fixed and annual energy costs. The applicability of developed method is illustrated with the help of a design example. It was found that the reliability of the branched network varied with total annual cost as well as the capital cost of the network for different sets of pipe diameters in the network. Further, it was found that the reliability for the designed network using total annual cost was higher than using capital cost. Therefore, the use of total annual cost should be preferred over the capital cost in the design to establish the balance between reliability and economy. The presented method provides an easy approach for water supply engineers to determine economical as well as reliable branched pipe networks.

Keywords—System reliability, reliability cost ratio, total annual cost.

1. INTRODUCTION

Water distribution system plays an important role in supplying water to consumers for different uses such as domestic, public, commercial and industrial. Therefore it is very important that the water distribution system should supply desired quality of water in required quantities with desired pressures to all consumers throughout the design period. The performance of system can be determined by estimating the reliability of water distribution system. In general, reliability is defined as the probability that the system will perform its function appropriately for a specified time period under given conditions. Reliability of water distribution system is decided according to the availability of water at source, transmission of water to treatment plants, treatment of raw water to the desired quality; and transmission, storage and distribution of the treated water. It is also important that quality water is made available to the consumers in the required quantities at desirable pressures throughout the design period.

In the traditional method of a pipe line design the energy is balanced against the loss of energy. In the optimization methods, the optimal solution is obtained by minimizing the cost of the network. In the recent past, efforts have been made by the researcher's to use heuristic methods like Genetic Algorithms (Simpson et al., 1994; Savic and Walters, 1997), nonlinear programming (Shamir 1974; Lansey and Mays 1989; Varma et al. 1997), Simulated Annealing (Cunha and Souse 1999), ant colony optimization (Maier et al. 2003). Further, in order to analyze the reliability of water distribution system, different approaches are presently being employed by researchers and analysts like (Rowell and Barnes 1982; Kettler and Goulter 1985). In the present study, reliability based design using total annual cost satisfying the minimum and maximum velocity requirements is presented to determine the best set of pipe sizes with desired reliability for different links of a branched water distribution network.

2. METHODOLOGY

The reliability based method for designing a branched pipe network involves computation of total annual cost of the network and system reliability as:

2.1 Pipeline Cost: The cost of a pipeline varies with diameter and annualized fixed cost of the pipe line can be obtained as:

$$F_c = C_r \times I_c \tag{1}$$

Where, I_c = Initial cost of the pipeline (Rs/m); C_r = Capital recovery factor which can be calculated as:

$$C_r = \frac{i(1+i)^n}{(1+i)^n - 1} \tag{2}$$

Where, i = Decimal equivalent annual interest rate; n= Life of the pipe (year).

2.2 Energy Cost: The annual energy cost for overcoming frictional head loss can be calculated as:

$$\mathrm{E_c} = \frac{73.5\mathrm{Q} \times \mathrm{h_f} \times \mathrm{t} \times \mathrm{C_e}}{75\eta} \tag{3}$$

Where, E_c = Annual energy cost (Rs); Q = Flow rate (liter/s); h_f= Frictional head loss of pipe (m); t = Annual use (hours); C_e= Cost of electricity (Rs/kW h); η=Efficiency of pump (%).

The value of head loss h_f can be calculated by the Darcy-Weisbach formula as:

$$h_f = \frac{f\,L\,V^2}{2\,g\,D} \tag{4}$$

Where, h_f = Frictional energy head loss (m); f = Darcy-Weisbach friction factor for pipe material (dimensionless); L= Length of pipe (m); D = Inside diameter of pipe (m); V = Mean velocity of flow through the pipe (m/s); g = Acceleration due to gravity (m^2/s).

The friction factor can be calculated using Swami and Jain (1976) formula:

$$f = \frac{0.25}{\left[\log_{10}\left(\frac{\varepsilon}{3.7d} + \frac{5.74}{Re^{\cdot 9}}\right)\right]^2} \tag{5}$$

Where, ε = Average height of roughness elements (m); R_e= Reynolds Number.

The value of R_e can be calculated as:

$$R_e = \frac{4Q}{\pi \vartheta D} \tag{6}$$

Where ϑ is the kinematic viscosity (m^2/s). In this study ε is taken as 0 .00025 m for cast iron pipes and the value of ϑ is taken as 10^{-6} m^2/s for water.

***2.3 Total Annual Cost**:* The total annual cost of a pipeline can be represented as sum of the annual fixed cost and annual energy cost:

$$T_c = F_c + E_c \tag{7}$$

2.4 Reliability

In reliability of water distribution networks, the working and closure times for pipes, pumps and valves can be obtained by considering availability and unavailability during the time interval of one year (Bhave, 2003). The working condition probability and the shutdown or closure probability of pipe, using the break rate N (y) $km^{-1}yr^{-1}$ for a pipe length L km for year y can be obtained by using failure rate F (t) of a pipe per year which depends on pipe break rate and can be obtained as:

$$F(t) = N(y) \times L \tag{8}$$

Using the failure rate and mean time to repair (MTTR), the closure and working times of a pipe, ratio of working time to total time i.e. probability of system element per year are calculated as:

$$\text{Closure time per year} = N(y)LT_r \quad (9)$$

$$\text{working time per year} = 365 - N(y)LT_r \quad (10)$$

$$\text{working condition probability per year } p_i = \frac{365 - N(y)LT_r}{365} \quad (11)$$

The system should be satisfactory to an acceptable level during the entire design period. It is considered the period of analysis as one year (365 days), the last year of design period. If the network has acceptable reliability level in this year, naturally it is acceptable for the earlier years.

2.4.1 Node reliability parameter or probability of node j can be defined as the product of working condition probability of pipes upstream of node j.

$$R_{nj} = \prod_{i=1}^{nlink} p_i \quad (12)$$

2.4.2 Volume reliability parameter: It is the ratio of total available outflow volume to required outflow volume for the entire network for all states during the period of analysis as:

$$R_v = \left(\frac{\sum_j V_j^{avl}}{\sum_j V_j^{req}}\right) = \left(\frac{\sum_j q_j^{avl} t_j}{\sum_j q_j^{req} t_j}\right) \quad (13)$$

Where, V_j^{avl} = available volume at demand node j; V_j^{req} = required flow at demand node j; q_j^{avl} = available discharge rate at demand node j; q_j^{req} = required discharge rate at demand node j; t_j = time duration for each demand node (same for all nodes).

2.4.3 System Reliability Parameter: To describe the reliability of a water distribution network by a single parameter called system reliability parameter (R_s) is proposed in analysis as:

$$R_s = R_v F_t F_n \quad (14)$$

Where, F_t= time factor; and F_n= node factor.

The time factor is defined as:

$$F_t = \frac{\sum_J P_J}{J} \quad (15)$$

where, J= total number of demand nodes.

The node factor is the geometric mean of the node reliability parameters and defined as:

The node factor is the geometric mean of the node reliability parameters and defined as:

$$F_n = \left(\prod_{j=1}^{J} R_{nj} \right)^{1/J} \tag{16}$$

2.5 Reliability cost ratio

Since the fixed cost increases with increase in the pipe sizes of a network, the reliability of the system also increases. However, the energy cost deceases with increase in pipe sizes. A satisfactory network can be selected by the ratio of reliability to total cost. Therefore to design a network that set of pipe sizes is selected which has largest value of reliability cost ratio.

3. DESIGN EXAMPLE AND DISCUSSION

A design example is presented to show the applicability of the developed reliability based method.

3.1 Example

A water distribution pipe network is to be designed for supplying water to a residential area from one source as shown in Figure 1. In designing a water distribution network the following conditions and data were used.

Design period = 30 years; daily use hours = 10; decimal equivalent annual interest rate = 10% ; efficiency of pump = 70%; cost of electricity C_e = Rs. 2.5/kW h; repair time = 2 days.

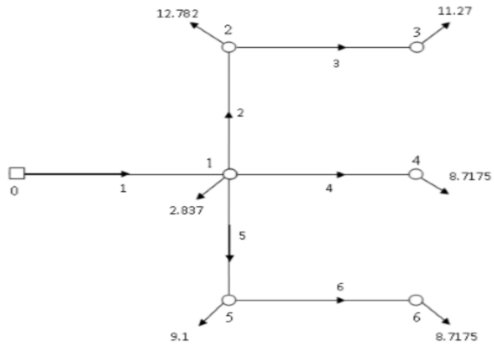

Figure 1: Branched network

The potential diameters and their unit costs of S and S centrifugally cast (spun) iron pipes (Class LA) used in network are given in Table 1 as applicable in rate analysis report of Public Works Department for block 87 Rudrapur (Udhamsingh nagar), Uttarakhand, India for the year 2014-2015. Pipe break rates taken from Bhave (2003) for different pipe sizes are given in Table 2. Pipe lengths, diameters and flow rates through each pipe are given in Table 3. Potential pipe sizes for each pipe link by considering the minimum and maximum velocity constraints are also given in Table 3.

The designer is interested in determining that combination of pipe sizes which results in the maximum value of the ratio of reliability to total annual cost for the distribution network.

3.2 Solution

The given data were used to calculate the total annual costs. Data from Table 1 were used to calculate total annual cost in Rs/m by Equation (7) for each pipe size. Pipe break rates from Table 2 were used to calculate reliability parameters of pipe network.

Table 1 Unit cost of available CI pipe sizes

S.No.	Pipe Diameter (mm)	Cost per unit length (Rs./m)
1	100	1075.6
2	125	1339.6
3	150	1598.1
4	200	2715
5	250	3543.4
6	300	4779.6
7	350	5728.9
8	400	7549.2
9	450	9141
10	500	10616.7
11	600	14845.7

Table 2 Break rate data for different pipe sizes

S.No.	Pipe Diameter (mm)	Break rate (breaks/km/yr)
1	100	1.36
2	150	1.04
3	200	0.71
4	250	0.39
5	300	0.07
6	350	0.05
7	400	0.05
8	450	0.04
9	500	0.04
10	600	0.04

The minimum and maximum permissible values of velocity were taken as 0.6 m/s and 2.5 m/s, respectively. Different possible sets of pipe network were made by changing the diameters of different links taken from Table 3. Different possible sets of diameters are given in Table 4. The system reliability and total annual cost were calculated for each set of pipe network.

Table 3 Flow rates in different pipe links and available potential pipe sizes.

Link No.	(U/S-D/S) Node	Length (m)	Flow rate (litre/s)	Pontential pipe size (mm)	Velocity (m/s)
1	0-1	1200	53.455	200	1.701
				250	1.088
				300	0.756
2	1-2	1100	24.0525	150	1.361
				200	0.765
3	2-3	1000	11.27	100	1.434
				150	0.637
4	1-4	1200	8.7175	100	1.109
5	1-5	1000	17.8475	100	2.272
				150	1.009
6	5-6	1100	8.7175	100	1.109

Table 4 Possible sets of pipe sizes of branched network

Set No.	Diameters (mm) for link number					
	1	2	3	4	5	6
I	300	200	150	100	150	100
II	300	200	100	100	150	100
III	300	200	150	100	100	100
IV	300	200	100	100	100	100
V	300	150	150	100	150	100
VI	300	150	100	100	150	100
VII	300	150	150	100	100	100
VIII	300	150	100	100	100	100
IX	250	200	150	100	150	100
X	250	200	100	100	150	100
XI	250	200	150	100	100	100
XII	250	200	100	100	100	100
XIII	250	150	150	100	150	100
XIV	250	150	100	100	150	100
XV	250	150	150	100	100	100
XVI	250	150	100	100	100	100
XVII	200	200	150	100	150	100
XVIII	200	200	100	100	150	100
XIX	200	200	150	100	100	100
XX	200	200	100	100	100	100
XXI	200	150	150	100	150	100
XXII	200	150	100	100	150	100
XXIII	200	150	150	100	100	100
XXIV	200	150	100	100	100	100

It was found that the ratio of reliability to total annual cost was maximum for set XXII which comprised of pipe sizes 200, 150, 100, 100, 150, 100 mm for link 1, 2, 3, 4, 5, 6, respectively. Similarly, it was found that the ratio of reliability to capital cost was maximum for set XXIV which comprised of pipe sizes 200, 150, 100, 100, 100, 100 mm for link 1, 2, 3, 4, 5, 6, respectively. The design results as the best set of pipe sizes for the network obtained by using two types of cost are given in Table 5

Table 5 Comparison of results for capital cost and total annual cost

Cost consideration	Set No.	Diameter (mm)	Reliability	Cost	Reliability cost ratio
Capital cost	XXIV	200	0.95969748	9640990	9.954×10^{-08}
		150			
		100			
		100			
		100			
		100			
Total annual cost	XXII	200	0.96139182	1359641.7	7.070×10^{-07}
		150			
		100			
		100			
		150			
		100			

From Table 5 it can be seen that in order to arrive at a more reliable network of pipes, total annual cost should be preferred in the reliability based design for calculating the ratio of reliability to cost.

4. CONCLUSIONS

The developed reliability based design method for branched networks can be used to obtain the economical network for the desired level of reliability by considering the permissible values of the minimum and maximum velocity. On comparing the ratio of reliability to cost, it was found that the use of total annual cost should be preferred over the capital cost in the design to establish the balance between reliability and economy.

REFERENCES

1. *Bhave (2003). Optimal design of water distribution networks. Narosa publishing house., New Delhi, India.*
2. *Cunha, M. C., and Sousa, J. (1999). Distribution network design optimization: Simulated annealing approach. J. Resour. Plann. Manage, 125 (4):215–221.*
3. *Kettler, A.J. and Goulter, I.C. 1985. An analysis of pipe breakage in urban water distribution networks. Canadian J. of Civil., Engrg., 12(2), 286-293.*

4. *Lansey, K., and Mays, L., 1989. Optimization Model for Water Distribution System Design. J. of Hydraul. Engrg. ASCE, Vol. 115, No. 10, pp. 1401-1418.*
5. *Maier, H. R., 2003. Ant colony optimization for the design of distribution systems. J. Resour. Plann. Manage.129 (3): 200–209.*
6. *Rowell, W.F. and Barnes, W.J. 1982. Optimal layout of water distribution systems. J. of Hydraulic Division., ASCE, 108 (1), 137-148*
7. *Savic, D.A., and Walters, G.A. 1997. Genetic algorithms for least-cost design of distribution networks. J. Resour. Plann. Manage, 123(2): 67-77.*
8. *Shamir, U. 1974. Optimal design and operation of water distribution systems. Water Resour. Res., 10(1), 27-36.*
9. *Simpson, A. R., Dandy, G. C., and Murphy, L. J. 1994. Genetic algorithms compared to other techniques for pipe optimization. J. Resour. Plann. Manage, 120 (4):423–443.*

Boundary Shear Stress Analysis in a Meandering Compound Channel

Debashish Khuntia[1], Saine S. Dash[2], Kishanjit K. Khatua[3],
[1]M.Tech Scholar, Dept. of Civil Engineering, National Institute of Technology, Rourkela-769008, India
[2]Ph.D Scholar, Dept. of Civil Engineering, National Institute of Technology, Rourkela-769008, India
[3]Associate Professor, Dept. of Civil Engineering, National Institute of Technology, Rourkela-769008, India
Email: debashish.rocky@gmail.com

A B S T R A C T

Distribution of boundary shear stress along the wetted perimeter directly affects the flow structure in an open channel flow. Also, the idea regarding boundary shear stress distribution provides solution to many hydraulic problems, such as understanding the mechanism of sediment transport, estimating conveyance of a channel bank erosion and channel migration problems. Prediction of boundary shear distribution in the meandering compound channel is critical in many engineering problems such as channel design, calculation of energy losses, and sedimentation. During the floods, part of the discharge passes through the main channel while the rest passes through the floodplains. For such meandering compound channels, the flow structure becomes complicated due to the transfer of momentum between the main channel and the adjoining floodplains which admirably disturbs the shear stress distribution among them. Based on the experimental results, this paper predicts the distribution of boundary shear carried by main channel and floodplain sub-sections of highly sinuous meandering compound channels. Thus, the objective is to calculate the percentage of shear force carried by the floodplain as well as the main channel with respect to the total boundary shear force which will cover for the better understanding on scouring and deposition patterns in meandering compound channels. The model is also validated using the software Conventional Estimation System.

Keywords—Boundary Shear Distribution, Meandering Compound Channel, Sinuosity, Flow Depth, Momentum Transfer.

1. INTRODUCTION

Boundary shear stress distribution over the wetted perimeter of the meandering compound channel is part of a complex problem, involving the influence of the turbulence, the shape of the cross-section and the boundary conditions. Although recent work, has considered the phenomenon of boundary shear stress distribution, there are still several unexplored aspects that merit consideration, as for example, the influence of Reynolds and Froude number on the secondary flow and hence in turn, on the boundary shear stress distribution. Traditionally investigations have been made in rectangular compound channels, and as a result, certain general characteristics are not sufficiently well understood. The boundary shear stress distribution in trapezoidal compound meandering channels should be different from those in rectangular compound channels on account of the side slope effect. An understanding of the flow in the compound meandering channel can lead to a calculation procedure for more complex geometries, which will include the effect of secondary flows. Complex cross- sections, on the other hand, have had little attention paid to them in the past. As a result, there are limited data available to form comprehensive design method and reliance is still placed upon the empirically derived equations. This is surprising, since natural channels are irregular in shape, and often consist of a deep channel with adjacent flood plain(s). Because of the lateral and vertical momentum transfer between the different depths, the flow conditions in such kinds of channel are more complex than those in a simple channel. Owing to the importance of such channels in the natural environment, a better understanding flow in complex channels is vital, and a scientific necessity. The boundary shear stress is obtained under accurate and comprehensive field measurements in a well-focused laboratory experimentation under steady flow conditions. It provides the information regarding the flow structure details and the lateral momentum transfer in meandering compound channel.

The momentum transfer concept in meandering compound channel is that center of the flow towards the side wall of a channel, or from the main channel to a flood plain affects the bottom shear stress distribution. The determination of the boundary shear stress distribution in the meandering compound channel is the aim of the present work and also numerical software 1D package CES developed by HR, Wallingford for estimating the boundary shear stress in compound meandering channels and then compare the result with experimental results. The lateral transfer of linear momentum at the channel/flood plain interface is a complex problem because of the existence of vortices and the nature of the flow condition near the wall, which affect the distribution of boundary shear stress. The boundary shear stress distribution helps to solve the hydraulic problems, like computation of bed form resistance, cavitation, side wall correction, channel migration and estimating the conveyance of channel bank erosion.

2. PREVIOUS INVESTIGATIONS

The maximum wall and bed shear stresses were first determined mathematically in laminar flow using finite difference methods and presented in graphs by Lane (1955). Since they were incorporated in a book by Chow (1959), the graphs have been widely used by practicing engineers. However, they are only approximations to the actual shear stress distributions, since no account was taken of secondary flow phenomena. Recently Cruff (1965) and Rajaratnam et al. (1969) have found higher values for the maximum bed shear stress. Rajaratnam also found that these distributions were Reynolds number dependent, and that for an aspect ratio greater than three, the effect of Reynolds number was significant. More recently, Knight et al. (1984a) non-dimensionalised the maximum bed shear stress results from their experiments in rectangular open channels and compared them with those obtained by Cruff and Rajaratnam.

Much effort has been directed towards a better understanding of the hydraulics of compound channel flows. Sellin (1964) and Zheleznyakov (1971) who first demonstrated in the laboratory the effect of these mechanisms, found that the most evident feature of the interaction phenomenon is the reduction of local and mean velocities in the main channel at flood plain depths just above bank-full depth. Ghosh et al. (1971,1974), Myers and Elsawy (1975) and Rajaratnam et al. (1981) measured the boundary shear stress distributions for different compound channels with symmetric and asymmetric flood plain zones and concluded that the transfer of momentum from the main channel to the flood plain produces a decrease in main channel boundary shear stress and an increase in flood plain shear stress. Myers (1978) attempted to quantify the momentum transfer between the main channel and flood plain expressing it as "apparent shear stress" acting at the imaginary interface plane by assuming a force balance between the weight component of the flow and the total measured shear stress. Elsawy et al. (1983) and Prinos et al. (1985) have used laser-Doppler anemometry to measure turbulence characteristics and velocity distribution in a compound channel and found that the direct measurement of boundary shear stress. This finding also verifies the indirect methods for measuring boundary shear stress (e. g. the Preston-tube technique) in the interaction zone, where an inner law is assumed. The empirical relationships derived by Knight et al. (1984a, 1985) and Flintham et al. (1988) for the percentage of the total shear force carried by the walls, the mean and maximum shear stresses in simple channels and ducts are useful from a practical design point of view. Ervine, Alan, Koopaei, and selling (2000) presented a useful method which predicts the boundary shear stress distribution for straight and meandering compound channel by considering the Navier-Stokes equation which includes lateral shear, secondary flows and bed friction. Khatua (2008) taken five parameters such as amplitude, sinuosity Sr, relative depth, aspect ratio and width ratio in meandering compound channel which is used to develop general equations representing the total shear force percentage carried by floodplain. Patnaik and Patra (2012) shows the effect of aspect ratio and sinuosity on the wall and bed shear forces and also determined the contribution of wall and bed shear to the total boundary shear force in the highly meandering channel. Pradhan and Khatua (2014) analysis the boundary shear stress and shear force distribution along the bed and side slopes throughout the meandering path of a highly sinuous meandering channel. These investigations give a fairly good indication of the existence of the secondary flow cells and that they have a significant influence on the boundary shear stress and primary velocity distributions. Although turbulence models have been moderately successful in their prediction of flow in compound channels, because of the complexity of the flow structures the non-uniform nature of the boundary shear stress distribution is neither uniquely related to the Reynolds number nor the geometry parameters of the channel. Thus the these non-uniformities is still heavily reliant upon reliable experimental data.

3. EXPERIMENTAL SETUP

In order to investigate the influence momentum transfer mechanism for the boundary shear stress distribution in meandering compound channels, several series of experiments were undertaken using the Preston tube technique. In addition, point velocities were measured across the whole cross-section for selected flow depths. Moreover, the interaction between the main channel and flood plain of a compound channel is also of particular interest.

The experiments were conducted in a 15m long tilting channel with a cross section 0.33m wide x 0.065m deep in Fluid Mechanics and Hydraulics Laboratory of NIT Rourkela. The channel was supported on a hydraulically jacked frame which could be rotated about a hinge joint beneath the entrance tank. The experimental channel was built inside the existing walls of the flume with Perspex sheet (6 to 10 mm thick) is used for the bed and wall of channel thick having Manning's n value=0.01. A compound trapezoidal section was first constructed with constant side slopes of 1: 1 and a constant bed width of 0.33m. By introducing side and bottom panels, compound channels were formed to give base widths of channel equal to 3.95m, thus giving aspect ratios, 2B/H >5. Water was supplied to the channel by an overhead tank through a 6 in. dia. Pipeline. To reduce large scale disturbances, and in order to ensure that the flow was uniformly distributed, a system of the stilling chamber was placed at the upstream end of the channel where the entrance tank and the bell-mouth shaped inlet transition section were located. Individual bell-mouth shaped transition sections were built for each sized trapezoidal channel and served to reduce separation and improved the development of the mean flow in the channel.

Table-1: Details of Geometrical Parameters of the Meandering Compound Channel

Sl.No.	Descriptions	Meandering compound channel
1	Type of main channel	Trapezoidal
2	Main channel bottom width (2b)	33cm
3	Bank full Depth of main channel	65mm
4	Top width of compound section (2B)	395cm
5	Side slope of main channel	1V:1H
6	Bed slope of the channel (S)	0.0011
7	Sinuosity (Sr)	1.11
8	Type of floodplains	Unsymmetrical
9	Flume size (l×b×h)	15m×4m×0.5m
10	Type of main channel	Trapezoidal

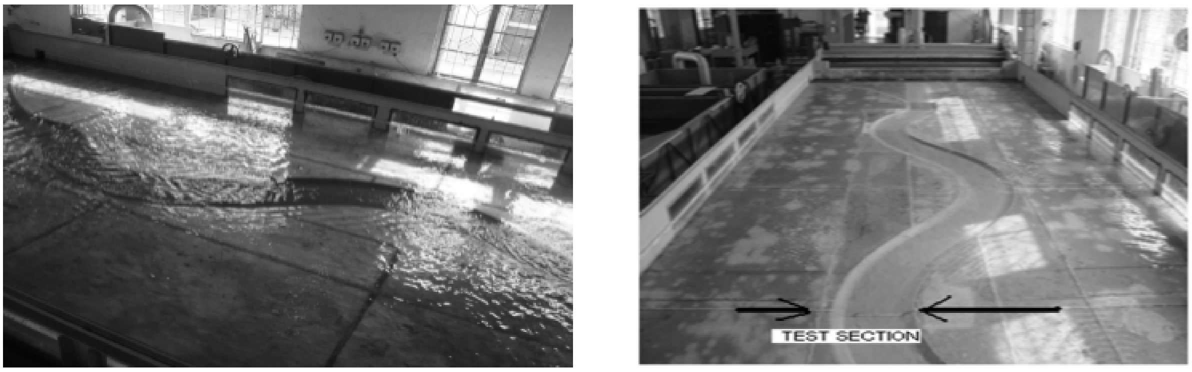

Figure 1. Photographs of the Experimental Channel

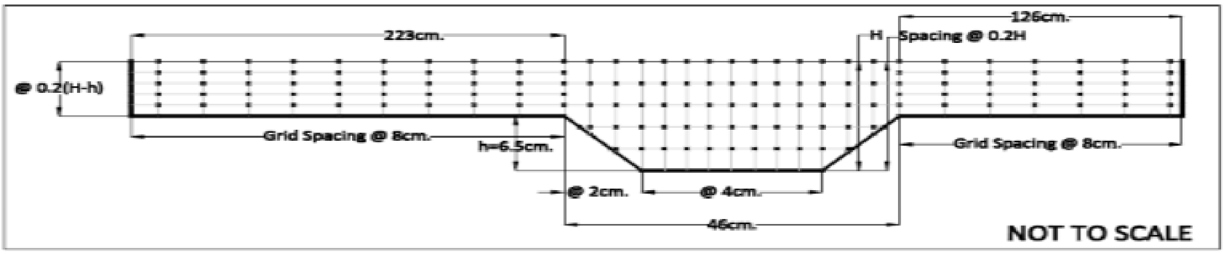

Figure 2. Grid Arrangement of Points for Shear Stress Measurement across the Channel Section.

3.1 Measurement of Boundary Shear Stress

There are several methods for determining the intensity of shear stress at a fixed boundary in fluid flow. One of the most simple and convenient methods is that developed by Preston (1953) for calculating boundary shear stress. He used a wall mounted circular Prandtl tube resting on the boundary, and deduced an expression connecting the dynamic pressure with the boundary shear stress. The method is based on the assumption of the inner law of the wall. Preston related the pressure difference between dynamic and ΔP to the independent variables ρ, υ, τ_0 and d to yield a relation of the form:

$$\left(\frac{\Delta P d^2}{4\rho\upsilon^2}\right) = F\left(\frac{\tau_0 d^2}{4\rho\upsilon^2}\right) \qquad (1)$$

where d is the outside diameter of the tube, ρ is the density of the flow, υ is the kinematic viscosity of the fluid, and F is an empirical function.

Since some controversy arises as to whether Preston's calibration (obtained in fully developed pipe flow) could be applied to external flows, many investigators have attempted to improve on the original calibration equation, e. g. Patel (1965), Head and Rechenburg (1962). The latter found evidence of some error in Preston's original calibration, and this led to Patel's extremely thorough investigation which was published in 1965. In Patel's calibration, the relationship between the two non-dimensional parameters which are used to convert pressure readings to boundary shear stress x* and y* was given as:

$$x^* = \log_{10}(\frac{\Delta P d^2}{4\rho \upsilon^2}) \text{ and } y^* = \log_{10}(\frac{\tau_0 d^2}{4\rho \upsilon^2}) \quad (2)$$

In the form

For $y^* < 1.5$ $\quad y^* = 0.5x^* + 0.037$ (3)

For $1.5 < y^* < 3.5$ $\quad y^* = 0.8287 - 0.1381x^* + 0.1437x^{*2} - 0.006\, x^{*3}$ (4)

For $3.5 < y^* < 5.3$ $\quad x^* = y^* + 2\log_{10}(1.95y^* + 4.10)$ (5)

In the present case, all shear stress measurements are taken in the meandering compound channel. By using pitot tube, the pressure reading was taken across the channel along the bed and side slopes. The differential pressure is calculated from the readings on the vertical manometer by,

$$\Delta P = \rho g \Delta h \quad (6)$$

where Δh is the pressure difference between the dynamic and static, g is the acceleration due to gravity and ρ is the density of water. Here the tube coefficient is taken as a unit and the error due to turbulence is considered negligible.

3.2 Shear Force Distribution

At each section the boundary shear stress is integrated over the wetted perimeter to get the shear force at the inner wall, outer wall and bed separately.

$$SF_{Floodplain} = \int_{Floodplain\ Bed} \tau dp + \int_{Floodplain\ Wall} \tau dp \quad (7)$$

$$SF_{Main\ Channel\ Wall} = \int_{Main\ Channel\ Wall} \tau dp \quad (8)$$

$$SF_{Bed} = \int_{Bed} \tau dp \quad (9)$$

$$SF_{Left\ Floodplain} + SF_{Left\ MC\ wall} + SF_{Bed} + SF_{Right\ MC\ wall} + SF_{Right\ Floodplain} = SF_{Total} \quad (10)$$

After finding the shear force distribution in different sections the boundary shear force distribution is plotted for each section and shown in figure 4.

4. RESULT AND DISCUSSION

The boundary shear stress distributions for the compound meandering channel are shown in Fig.3. There are different flows regions are shown in Fig 3 such as left floodplain walls, left floodplain bed, main channel wall, main channel bed along with right floodplain wall and right floodplain bed. Due to meandering compound channel, the left floodplain has large width and right floodplain has smaller width. Here, the boundary shear stress gradually increases from the far end of left floodplain towards the main channel. Likewise, at the right floodplain the boundary shear stress falls sharply and after some distance the shear stress moderate fall towards the floodplain end. In the main channel wall is seen that the maximum shear at the inner wall and lower shear stress at the outer wall as compared the inner wall. When depth of flow increases, it is shown that the boundary shear stress magnitude is dependent on depth of flow in the meandering compound channel. In meandering compound channel the flow mechanisms are being complex (Ervine et al. 2000; Shiono and Muto, 1998). It is very difficult to obtain any fixed pattern in the boundary shear stress variation for meandering compound channel flow depths considered in the present study (Figs.5).

From the boundary shear force distribution diagram it is observed that the left and right floodplain shares maximum percentage of shear force. With increase in flow depth the shear force shared by each floodplain increases. It can be easily seen that left floodplain shares more shear force than the right floodplain. This is primarily due to different widths of each floodplain. With increase in depth of flow percentage of shear force shared by main channel bed increases while that of the main channel walls decreases. At lower depth left wall of main channel comparatively shares more shear force than the right wall. But with increase in flow depth the difference between the percentage of shear force shared by both the walls of main channel decreases and at higher depths shared shear force percentage for both the walls becomes nearly equal.

CES (Conveyance Estimation System) was used to predict the distribution of boundary shear stress across their wetted perimeter of the experimental channel to examine the suitability of the numerical tools used in the software, in validating a large scale flume with wide floodplain as used in the research. As regards simulation through CES, because of smooth main channel and floodplains of NIT channels, for meandering channels were simulated keeping the roughness value in the main channel and floodplains in *.RAD file near to 0.01which is same as that of the experimental channel. Thus the results for the distribution boundary shear across the cross section of compound sections for various floodplain flow cases were extracted from CES. The distribution of point boundary shear stress (τ) over the wetted perimeter of the whole compound section is presented. The boundary shear stress (τ) is normalized with maximum shear stress (τmax) and is shown in Fig.5 for the meandering compound channel. A comparative picture was then formulated to observe the difference in the results obtained through numerical tools visa via the experimental observations. The results from the numerical tool are found to be in sync with the experimental results. The trend of boundary shear stress in both the methodology shows similarities. In left floodplain, boundary shear stress increases smoothly towards the interface between the floodplain and main channel. There is a sharp fall in the boundary shear stress on the right interface from the main channel towards the right floodplain.

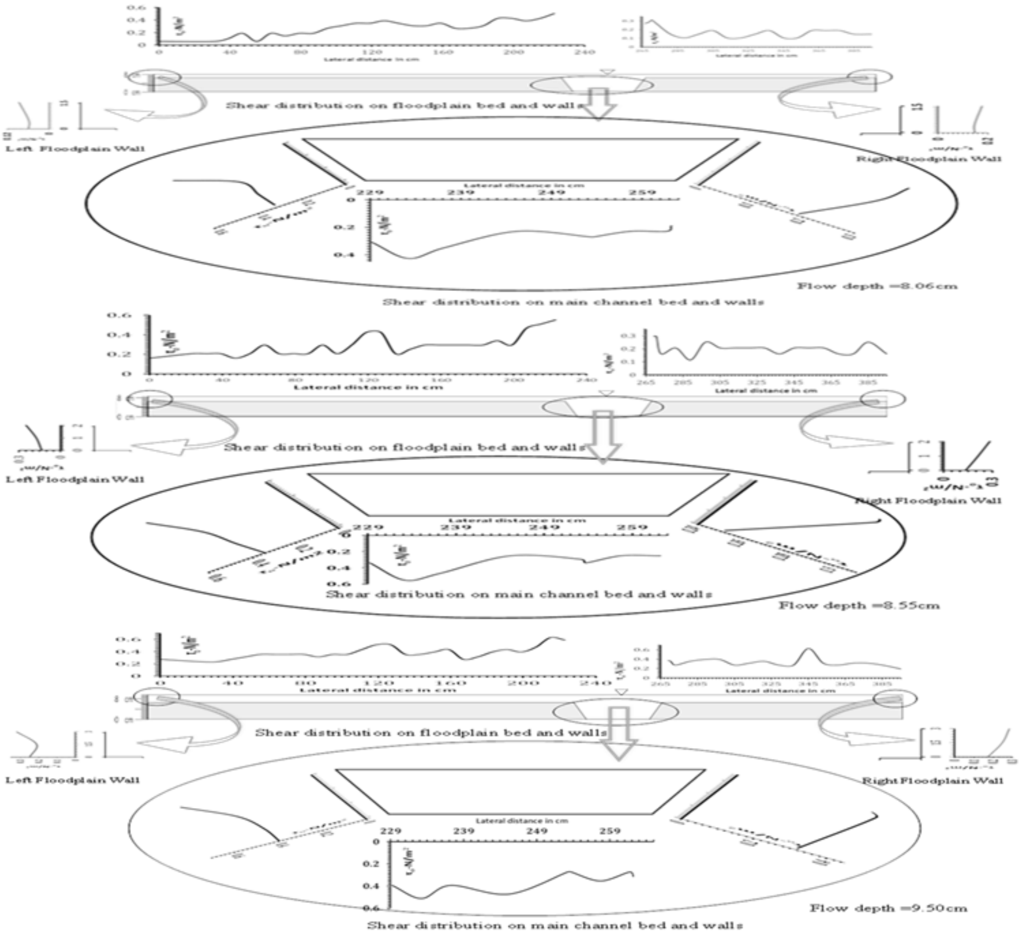

Figure 3 Boundary shear stress distributions in meandering compound channel for different depth of flows

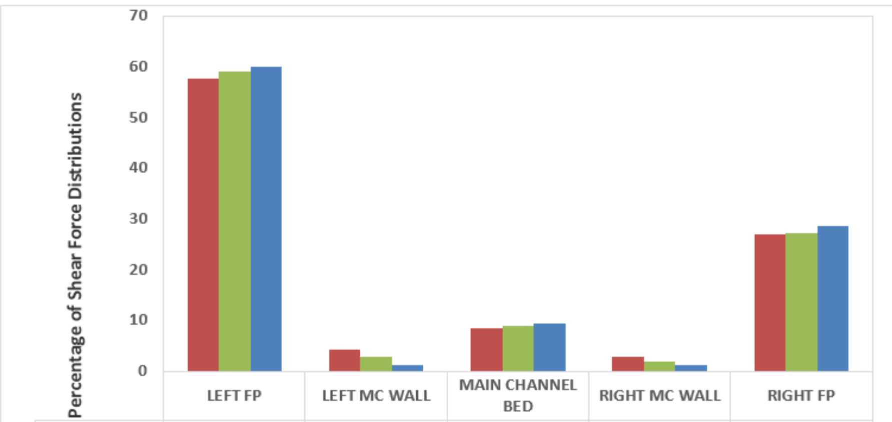

	LEFT FP	LEFT MC WALL	MAIN CHANNEL BED	RIGHT MC WALL	RIGHT FP
Depth 8.06cm	57.60343141	4.258954078	8.47161803	2.824746677	26.8412498
Depth 8.55cm	59.05540262	2.905084038	9.004078046	1.804205997	27.2312293
Depth 9.5cm	59.85565508	1.117876207	9.338681172	1.123039553	28.56474799

Figure 4 % of Shear Force Distribution in Meandering Compound Channel for different sections

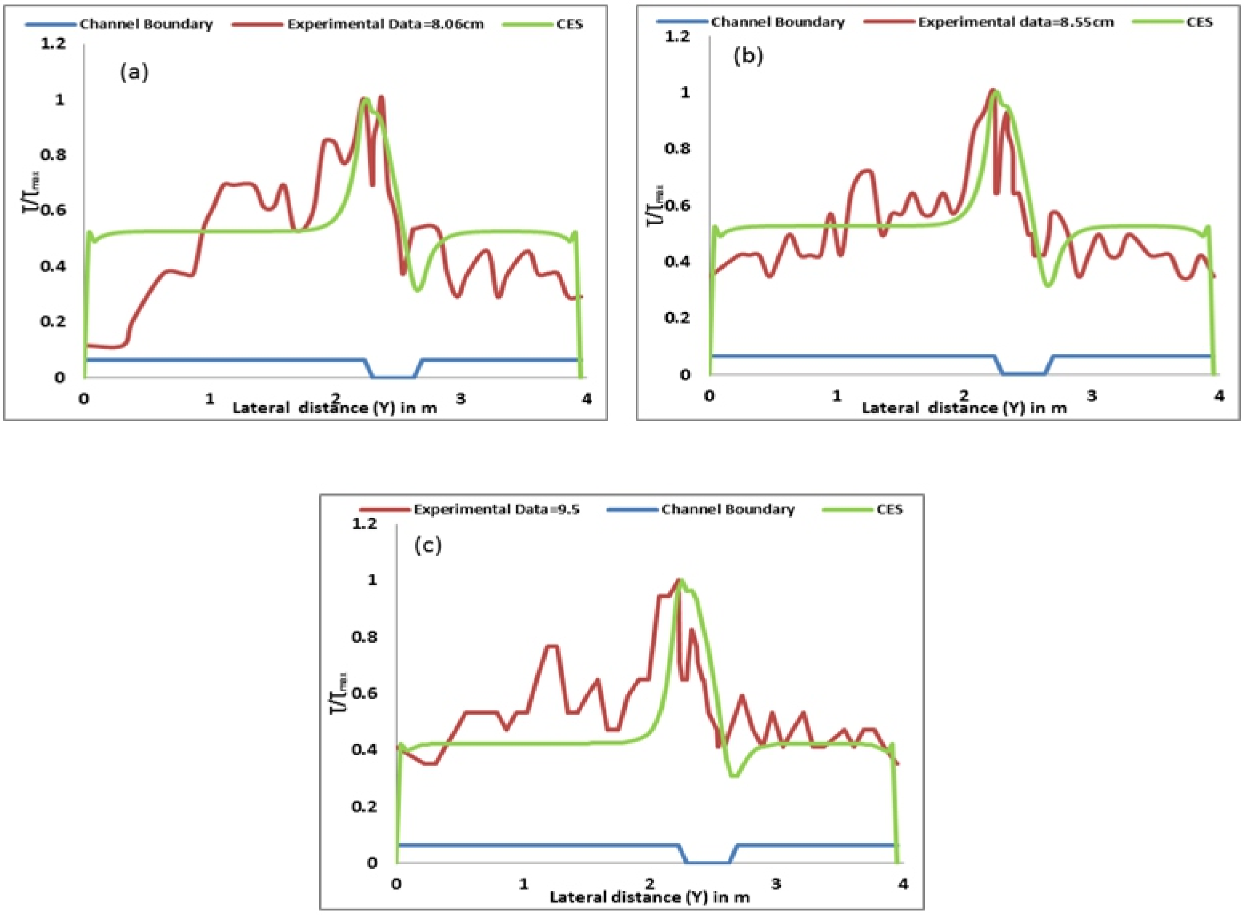

Figure 5 Comparisons with Boundary shear stress with CES for different depth of flow

5. CONCLUSIONS

- The boundary shear stress distribution over the wetted perimeter of the wide meandering compound channel for different flow depths have been shown to be markedly non-uniform, although the pattern in the main channel that the highest magnitude of resistance to the flow always occurs at the inner side of the bend.
- With increase in depth of water flow the percentage of boundary shear force shared by the each floodplain increases. The left floodplain accounts for around 60% sharing of shear force while the right floodplain accounts for nearly 28%.This is mainly because of the different widths of the floodplain.
- Percentage of shear force shared by main channel bed increases with flow depth while for the main channel walls it decreases. With increase in depth the difference between shear forces shared by the inner and outer main channel wall decreases and finally becomes nearly equal.
- The 1D software package 'Conveyance Estimation System' is capable of predicting the boundary shear distribution across the flow cross sections of the present wide meandering compound channel.

- The results from the numerical tool is found to be in sync with the experimental results. In left floodplain, boundary shear stress increases smoothly towards the interface between the floodplain and main channel. There is a sharp fall in the boundary shear stress on the right interface from the main channel towards the right floodplain. However, in case of the simulation studies conducted, it is observed that the CES package under predicted the observed values in most cases.

REFERENCES

Chow, V. T. (1959), Open Channel Hydraulics, McGraw-Hill, 1959, pp. 168-170.

Conveyance Estimation System v2.0 (2007) Wallingford Software, HR Wallingford OX10 8BAUK. http://www.river-conveyance.net/download.asp.

Cruff R. W (1965). Cross-channel transfer of linear momentum in smooth rect. Channel. U. S. Geol. Survey, Water-supply paper, vol. 1592, part B, B1-B26.

Elsawy, E. M., McKee, M. P. & McKeogh, E. J. (1983). Application of LDA Techniques to velocity and turbulence measurements in open channel of compound section. Proc. Int. Conf. I. A. R. E., vol. IBI, Moscow, Sept., 1983, pp. 255-263.

Ervine, D. A., Koopaei K. B. and Sellin R. H. J. (2000). Two Dimensional Solution for Straight and Meandering Over-bank Flows. J. Hydraul. Eng., ASCE, 126 (9), 653-669.

Flintham, T. P. and Carling, P. A. (1988). The prediction of mean bed and wall boundary shear in uniform and compositely rough channels. Int. Conf. on River Regime, edited by W. R. White, 1988, Published by John Wiley & Sons Ltd.

Ghosh, S. N and Jena, S. B (1971). Boundary shear distribution in open channel compound. Proc. ICE., vol. 49, Aug., 1971, pp. 417-430.

Ghosh, S. N. and Mehta, P. J. (1974). Boundary shear distribution in a compound channel with varying roughness distribution. Proc. ICE., vol. 57, Dec., 1974, pp. 159-163.

Khatua,K.K,(2008) Interaction of flow and estimation of discharge in two stage meandering compound channels. Ph.D Thesis Presented to the National Institute of Technology, Rourkela.

Knight, D. W., Demetriou, J. D. and Hamed, M. E. 1984a. Boundary shear in smooth rectangular channels J. Hyd. Engg.,, ASCE., vol. 110, No. 4, April 1984, pp. 405-422.

Knight, D. W. and Patel, H. S. (1985).Boundary shear in smooth rectangular ducts. J. Hyd. Engg.,, ASCE., vol. Ill,, No. 1, pp. 29-47.

Lane, E. W. (1955) Design of stable channels. Trans. ASCE., vol. 120, pp. 1234-1260.

Myers, W. R. C. & Elsawy, E. M. (1975).Boundary shear in channel with flood plain. J. Hyd. div. , Proc. ASCE., vol. 101, No. HY7, July, pp. 933-946.

Myers, W. R. C. (1978).Momentum transfer in a Compound Channel. Journal of Hydraulic Research. IAHR, vol. 16, No. 2,1978, pp. 139-150.

Patel, V. C (1965) Calibration of Preston tube and limitations on its use in pressure gradients. J. Fluid Mech., vol. 23, part 1, pp. 185-208.*

Patnaik, M., Patra.K.C., Khatua, K.K., Mohanty, L. (2013) Modeling Boundary Shear Stress in Highly Sinuous Meandering Channels. ISH Journal of Hydraulic Engineering, Taylor & Francis Group, UK.

Pradhan, A., Khatua,K.K., and Dash,S.S, (2014), Boundary Shear Force Distribution Along Different Reaches Of A Highly Meandering Channel. International Journal of Scientific Engineering and Technology, Issue Special.

Preston, J. H. (1953) The determination of turbulent skin friction by means of Pitot tubes, J. Royal Aero. Soc., vol. 58, Feb., pp. 109-121.

Engg., Proc. ASCE., vol. Ill,, No. 9. Sept., pp. 1246-1261.

Rajaratnam, N. & Ahmadi,, R. (1981) Hydraulics of channel with flood-plains. J. Hyd. Res. & I. A. H. R., vol. 19, No. 1,1981, pp. 43-60.

Rajaratnam, N. and Muralidhar, D. (1969) Boundary shear stress distribution in rectangular open channel. La Houille Blanche, No. 6, pp. 603-608.

Sellin, R. H. J. (1964). A laboratory investigation into the interaction between the flow in the channel of a river and that over its flood plain. La Houille Blanche, No. 7, 1964: pp. 753-801.

Shiono, K., Muto, Y. (1998).Complex flow mechanisms in compound meandering channels with overbank flow. J. Fluid Mech., Cambridge University Press.UK, 376, 22-261.

Zheleznyakov, G. V. (1971). Interaction of Channel and flood- plain streams. I. A. H. R. Conf. Paris, vol. 5, paper A302.

Instructions for Authors

Essentials for Publishing in this Journal

1 Submitted articles should not have been previously published or be currently under consideration for publication elsewhere.

2 Conference papers may only be submitted if the paper has been completely re-written (taken to mean more than 50%) and the author has cleared any necessary permission with the copyright owner if it has been previously copyrighted.

3 All our articles are refereed through a double-blind process.

4 All authors must declare they have read and agreed to the content of the submitted article and must sign a declaration correspond to the originality of the article.

Submission Process

All articles for this journal must be submitted using our online submissions system. http://enrichedpub.com/ . Please use the Submit Your Article link in the Author Service area.

-

Manuscript Guidelines

The instructions to authors about the article preparation for publication in the Manuscripts are submitted online, through the e-Ur (Electronic editing) system, developed by **Enriched Publications Pvt. Ltd**. The article should contain the abstract with keywords, introduction, body, conclusion, references and the summary in English language (without heading and subheading enumeration). The article length should not exceed 16 pages of A4 paper format.

Title

The title should be informative. It is in both Journal's and author's best interest to use terms suitable. For indexing and word search. If there are no such terms in the title, the author is strongly advised to add a subtitle. The title should be given in English as well. The titles precede the abstract and the summary in an appropriate language.

Letterhead Title

The letterhead title is given at a top of each page for easier identification of article copies in an Electronic form in particular. It contains the author's surname and first name initial .article title, journal title and collation (year, volume, and issue, first and last page). The journal and article titles can be given in a shortened form.

Author's Name

Full name(s) of author(s) should be used. It is advisable to give the middle initial. Names are given in their original form.

Contact Details

The postal address or the e-mail address of the author (usually of the first one if there are more Authors) is given in the footnote at the bottom of the first page.

Type of Articles

Classification of articles is a duty of the editorial staff and is of special importance. Referees and the members of the editorial staff, or section editors, can propose a category, but the editor-in-chief has the sole responsibility for their classification. Journal articles are classified as follows:

Scientific articles:

1. Original scientific paper (giving the previously unpublished results of the author's own research based on management methods).

2. Survey paper (giving an original, detailed and critical view of a research problem or an area to which the author has made a contribution visible through his self-citation);

3. Short or preliminary communication (original management paper of full format but of a smaller extent or of a preliminary character);

4. Scientific critique or forum (discussion on a particular scientific topic, based exclusively on management argumentation) and commentaries. Exceptionally, in particular areas, a scientific paper in the Journal can be in a form of a monograph or a critical edition of scientific data (historical, archival, lexicographic, bibliographic, data survey, etc.) which were unknown or hardly accessible for scientific research.

Professional articles:

1. Professional paper (contribution offering experience useful for improvement of professional practice but not necessarily based on scientific methods);
2. Informative contribution (editorial, commentary, etc.);
3. Review (of a book, software, case study, scientific event, etc.)

Language

The article should be in English. The grammar and style of the article should be of good quality. The systematized text should be without abbreviations (except standard ones). All measurements must be in SI units. The sequence of formulae is denoted in Arabic numerals in parentheses on the right-hand side.

Abstract and Summary

An abstract is a concise informative presentation of the article content for fast and accurate Evaluation of its relevance. It is both in the Editorial Office's and the author's best interest for an abstract to contain terms often used for indexing and article search. The abstract describes the purpose of the study and the methods, outlines the findings and state the conclusions. A 100- to 250-Word abstract should be placed between the title and the keywords with the body text to follow. Besides an abstract are advised to have a summary in English, at the end of the article, after the Reference list. The summary should be structured and long up to 1/10 of the article length (it is more extensive than the abstract).

Keywords

Keywords are terms or phrases showing adequately the article content for indexing and search purposes. They should be allocated heaving in mind widely accepted international sources (index, dictionary or thesaurus), such as the Web of Science keyword list for science in general. The higher their usage frequency is the better. Up to 10 keywords immediately follow the abstract and the summary, in respective languages.

Acknowledgements

The name and the number of the project or programmed within which the article was realized is given in a separate note at the bottom of the first page together with the name of the institution which financially supported the project or programmed.

Tables and Illustrations

All the captions should be in the original language as well as in English, together with the texts in illustrations if possible. Tables are typed in the same style as the text and are denoted by numerals at the top. Photographs and drawings, placed appropriately in the text, should be clear, precise and suitable for reproduction. Drawings should be created in Word or Corel.

Citation in the Text

Citation in the text must be uniform. When citing references in the text, use the reference number set in square brackets from the Reference list at the end of the article.

Footnotes

Footnotes are given at the bottom of the page with the text they refer to. They can contain less relevant details, additional explanations or used sources (e.g. scientific material, manuals). They cannot replace the cited literature.
The article should be accompanied with a cover letter with the information about the author(s): surname, middle initial, first name, and citizen personal number, rank, title, e-mail address, and affiliation address, home address including municipality, phone number in the office and at home (or a mobile phone number). The cover letter should state the type of the article and tell which illustrations are original and which are not.

<u>**Address of the Editorial Office:**</u>

Enriched Publications Pvt. Ltd.
S-9,IInd FLOOR, MLU POCKET,
MANISH ABHINAV PLAZA-II, ABOVE FEDERAL BANK,
PLOT NO-5, SECTOR -5, DWARKA, NEW DELHI, INDIA-110075,
PHONE: - + (91)-(11)-45525005

Notes: